

CHAPTER 6

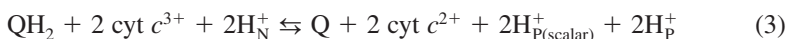
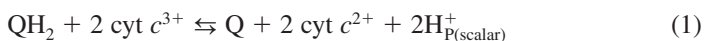
The bc_1 Complex: What is There Left to Argue About?

ANTONY R. CROFTS

Department of Biochemistry,
University of Illinois at Urbana-Champaign,
419 Roger Adams Lab,
600 S. Mathews Avenue,
Urbana,
IL 61801

1 Introduction

The cytochrome bc_1 complex and its relatives are the central enzymes of respiratory and photosynthetic chains, and catalyze the oxidation of hydroquinones in the membrane by small mobile aqueous redox proteins. The redox work is coupled to transfer of protons across the membrane. For the bc_1 complex, which oxidizes ubiquinol (quinol, QH_2), the reaction equations can be written to represent the overall reaction by its scalar and vectorial components:



The mechanism through which this overall reaction is accomplished has been the subject of extensive work from many labs, which has led to a consensus represented by a modified Q-cycle¹⁻³ (Figure 1, see⁴ for a historical review). The mechanism appears at first sight to be so complicated as to discourage detailed physicochemical description. As the structures have shown,⁵⁻⁸ the three catalytic subunits contain five catalytic interfaces, three of them concerned with processing external substrates, and these are connected through two separate-electron transfer chains. The complex is a homodimer, and much speculation about interaction between monomers has opened the possibility of even higher levels of complexity.^{7, 9-14}

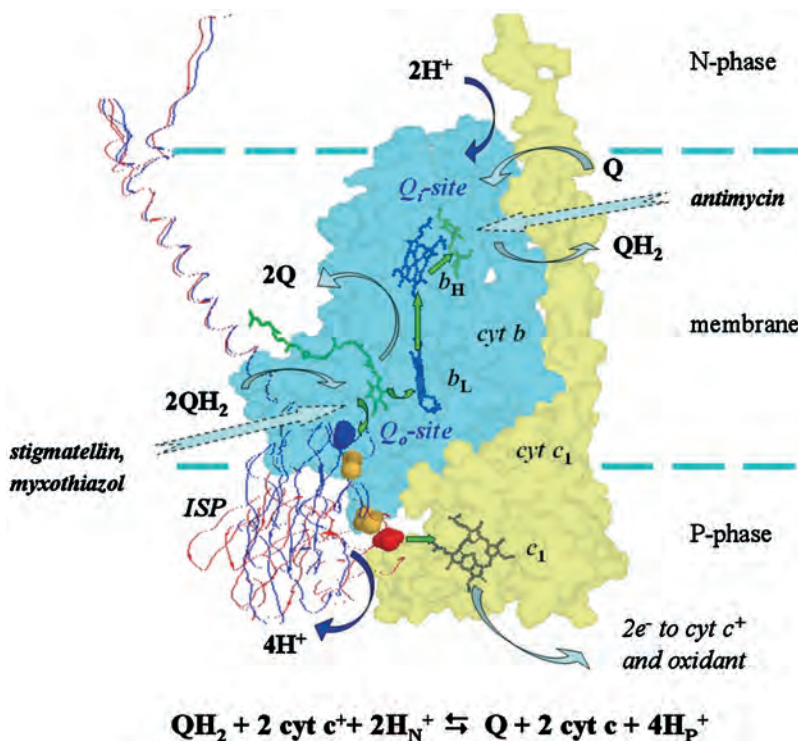


Figure 1 The modified *Q*-cycle shown in the context the structure. The three catalytic subunits of a functional monomer of the *bc*₁ complex (PDB 2bcc) from chicken mitochondria are shown with a quinol modeled in the *Q*_o-site to replace stigmatellin, and quinone at the *Q*_i-site. The *cyt b* subunit is shown by its transparent cyan surface, and the *cyt c*₁ subunit by a transparent yellow surface. The Rieske iron sulfur protein is shown as a ribbon cartoon, docked at the *b*-interface (blue) or at the *c*-interface (red). The approximate position of the membrane is shown by the dashed lines. The *b*-hemes are shown in blue, heme *c*₁ in green. The [2Fe-2S] clusters are shown as spacefilling models, colored as for the protein. Two additional positions for the cluster are shown (in CPK colors) to indicate the trajectory of movement between *b*- and *c*-interfaces. Binding and unbinding of quinone species, and docking of *cyt c*, are shown by broad curved arrows (gray-blue). Electron transfers are shown by small green arrows, *H*⁺ release and uptake are shown by curved blue arrows. The sites of action of inhibitors are shown by dotted gray arrows. For each turnover, two *QH*₂ molecules are oxidized to *Q* at the *Q*_o-site, and two successive electrons are passed down the pathways indicated. The two electrons going down the high-potential chain (ISP, *cyt c*₁, *cyt c*) are passed to a terminal oxidant. The two electrons going through the *b*-heme chain reduce *Q* to *QH*₂ at the *Q*_i-site through a two-electron gate, with storage of one electron as a *SQ* at the site. The modified *Q*-cycle in this form predated the structure by ~10 years, and the alignment here brings out the structural predictive power of the kinetic studies leading to the scheme

In this review, I want to show that this complicated mechanism can be presented in terms of simple partial processes representing kinetic steps. For each of these, the parameters for a formal description (rate constants, equilibrium constant, activation barrier, *etc.*) can be measured, or constrained to well-defined ranges. For the critical

rate-determining reaction, the bifurcated reaction leading to oxidation of QH_2 at the Q_o -site, we can offer a detailed description that explains the general properties, and several anomalous features that have been identified as problematic by other workers.

The Q-cycle mechanism appears to be essentially the same (with changes in parameters appropriate to species difference, *etc.*) whether observed in the isolated complex, in the mitochondrial respiratory chain, or in bacterial respiratory or photosynthetic chains. The photosynthetic bacteria offer many experimental advantages, and much of the work providing the formal descriptions presented here has been done in these systems, where turnover can be initiated *in situ* by activation of the photosynthetic chain. A brief saturating flash drives the photochemical reaction centers (RC) to generate the substrates for the bc_1 complex in $<10 \mu\text{s}$. In both *Rhodobacter* species commonly used, the stoichiometry of the photosynthetic chain ($\sim 2 \text{ RC}/bc_1$ complex) is such that, under uncoupled conditions, each bc_1 complex turns over once in returning the system to the initial state. The kinetics of electron transfer associated with turnover can be followed spectrophotometrically by watching the elementary redox events associated with each of the three heme centers and RC, which have distinct spectra. In addition, electrochromic responses of carotenoid pigments of the light-harvesting complex make it possible to measure the electrogenic events associated with turnover, facilitating exploration of the relation between electron transfer and protonpumping (reviewed in¹⁵). Dissection of the partial processes has been facilitated by inhibitors that bind specifically at either of the two quinone-processing sites. These can be used to limit the set of partial reactions and simplify interpretation. In addition, the use of redox potentiometry¹⁶ makes it possible to poise the system so that the effects of change in substrate concentration can be assayed over a wide range. Using these approaches, the modified Q-cycle was dissected into partial processes as summarized in Table 1. The rate and equilibrium constants shown are essentially those from work in the 1980s,^{1, 17–25} updated where more complete data are now available.

A remarkable feature of the work from the 1980s was the demonstration that the equilibrium constants calculated from measurements of E_m values accounted for the dynamic distribution of electrons in the antimycin-inhibited complex (Fig. 2). The initial concentrations of substrate could be varied through reduction of the quinone pool, or by applying one or two saturating flashes, and the metastable state established 10–100 ms after each flash was then measured and the electron distribution compared to that expected from E_m values. In the context of measured stoichiometries and the linked electrogenic processes, a match was found, but only for a particular formulation of the basic Q-cycle^{2, 3, 26–28} that had been largely ignored.^{1, 4, 29, 30} The modified Q-cycle emerging from this work has stood the test of time,³¹ and will be our basis for further discussion. Recent work from Osyczka *et al.*³² has extended the equilibrium approach developed in this earlier work to analysis of the behavior in mutant strains in which the redox chains have been further truncated by mutagenesis.

One important conclusion from this extensive set of data is that the thermodynamic driving forces for the different partial processes are not markedly modified by hidden interactions; there was no evidence for long-range control of electron transfer by conformational or allosteric interactions.^{18, 31, 32} A few qualifications are necessary:

- (i) Direct measurement of electron exchange between hemes b_H and b_L in response to the transmembrane electric field generated by the photochemical reactions

Table 1 Partial reactions of the bc_1 complex and their parameters

#	Reaction	$\tau/\mu\text{s}$	$\Delta G^\circ/\text{meV}$	K_{eq}	$\Delta E^\circ/\text{kJ}\cdot\text{mol}^{-1}$	Refs.
<i>Bifurcated reaction at Q_o-site</i>						
<i>a</i>	$2(\text{QH}_2 + \text{E}\cdot\text{ISP}_{\text{ox}}\cdot b_{\text{L}}\cdot b_{\text{H}} \rightleftharpoons \text{Q} + \text{E}\cdot\text{ISPH}\cdot b_{\text{L}}\cdot b_{\text{H}} + \text{H}_p^+)$	~ 770	-20	3	60-64	1, 15, 17-20, 4, 31, 166
<i>b-heme chain</i>						
<i>b</i>	$2(\text{E}\cdot b_{\text{L}}\cdot b_{\text{H}} \rightleftharpoons \text{E}\cdot b_{\text{L}}\cdot b_{\text{H}}^-)$	≤ 100	-130 (-60)	-160 (10)	<40	21-23, 33
<i>Q_r-site</i>						
<i>c</i>	$\text{E}\cdot b_{\text{L}}\cdot b_{\text{H}} + \text{Q} \rightleftharpoons \text{E}\cdot b_{\text{L}}\cdot b_{\text{H}}\cdot \text{Q}_1$	<200	-94	40		23, 117
<i>d</i>	$\text{E}\cdot b_{\text{L}}\cdot b_{\text{H}}\cdot \text{Q}_1 \rightleftharpoons \text{E}\cdot b_{\text{L}}\cdot b_{\text{H}}\cdot \text{SQ}_1^-$	<200	-50	7		52, 118,
<i>e</i>	$\text{E}\cdot b_{\text{L}}\cdot b_{\text{H}}\cdot \text{SQ}_1^- + 2\text{H}_N^+ \rightleftharpoons \text{E}\cdot b_{\text{L}}\cdot b_{\text{H}}\cdot \text{QH}_2$	<200	-168	703		119
<i>f</i>	$\text{E}\cdot b_{\text{L}}\cdot b_{\text{H}}\cdot \text{QH}_2 \rightleftharpoons \text{E}\cdot b_{\text{L}}\cdot b_{\text{H}} + \text{QH}_2$	<200	212	0.00025		
	<i>sum</i> $2 \text{E}\cdot b_{\text{L}}\cdot b_{\text{H}}^- + \text{Q} \rightleftharpoons 2 \text{E}\cdot b_{\text{L}}\cdot b_{\text{H}} + \text{QH}_2$	≤ 200	-100	50	<40	
<i>High potential chain</i>						
<i>g</i>	$2(\text{E}\cdot\text{ISPH}\cdot c_1^{2+} + \text{cyt } c^{3+} \rightleftharpoons \text{E}\cdot\text{ISPH}\cdot c_1^{3+} + \text{cyt } c^{2+})$	150	-70	15.4	28	17, 20, 31, 93
<i>h</i>	$2(\text{E}\cdot\text{ISPH}\cdot c_1^{3+} \rightleftharpoons \text{E}\cdot\text{ISP}_{\text{ox}}\cdot c_1^{2+} + \text{H}_p^+)$	10	20	0.46	18	116
<i>i</i>	<i>sum</i> $2(\text{E}\cdot\text{ISPH} + \text{cyt } c^{3+} \rightleftharpoons \text{E}\cdot\text{ISP}_{\text{ox}} + \text{cyt } c^{2+} + \text{H}_p^+)$		-50	7		
<i>Overall reaction</i>						
	$\text{QH}_2 + 2 \text{cyt } c^{3+} + 2\text{H}_N^+ \rightleftharpoons \text{Q} + 2 \text{cyt } c^{2+} + 4\text{H}_p^+$		-500 (-2 Δp)		60-64	

Notes:

Rates are given as lifetimes, τ , which for 1st-order processes are $1/k_{\text{cat}}$. The value for reaction *a* is from the rate measured at $E_{\text{h},7} \sim 100$ mV (Q_{pool} 30% reduced), and represent about 80% V_{max} , obtained from extrapolation.²⁴ Values for ΔG° are given in meV ($\Delta G^\circ/F = -z\Delta E^\circ$), and calculated from measured E° values, as follows: for cyt c_2 , $E_{\text{m},7} = 340$ mV; for cyt c_1 , $E_{\text{m},7} = 270$ mV; for ISP, $E_{\text{m},7} = 290$ mV; for heme b_{L} , $E_{\text{m},7} = -90$ mV; for heme b_{H} , $E_{\text{m},7} = 40$ mV; for Q/QH_2 (pool), $E_{\text{m},7} = 90$ mV.^{18,28,120-122} Activation energies are taken from Arrhenius plots.⁹³

Reaction *a*: $\Delta G^\circ = -F(E_{\text{ISP}}^{\text{ox}} + E_{\text{heme } b_{\text{L}}}^{\text{ox}}) - 2 E_{\text{Q/QH}_2}^{\text{ox}}$.

Reaction *b*: Values in parentheses reflect heme b_{L} , $E_{\text{m},7} \sim -20$ when heme b_{H} charge is absent.³⁴

Q_r -site (reactions *c*, *d*, *e*, *f*): The properties of the Q_r -site were modeled using the following values: $[\text{bc}_1 \text{ complex}] = 60$ mM; $[\text{bc}_1 \text{ complex}] = 1$ mM; $K_{\text{QH}_2}^{\text{ox}} = 4000 \text{ M}^{-1}$; $K_{\text{Q}}^{\text{ox}} = 40 \text{ M}^{-1}$; for bound Q/QH_2 , $E_{\text{m},7} = 149$ mV; for bound SQ/QH_2 , $E_{\text{m},7} = 90$ mV; for bound SQ/QH_2 , $E_{\text{m},7} = 208$ mV; $pK(\text{heme } b_{\text{H}}) = 7.8$; $pK(\text{QH}^\bullet) = 12.5$. Other parameters were calculated using the formalism in.^{52,123,124} A Visual Basic program for modeling the site is available on request from the author.

enabled Shinkarev *et al.*³³ to explore the equilibrium constant under conditions in which only a single electron populated the chain, which was isolated from input or output by inhibitors. This worked confirmed an earlier suggestion,³⁴ that the measured redox potential of heme b_L reflected both an intrinsic E_m and an interaction with ferroheme b_H , likely coulombic in nature. The apparent E_m when heme b_H was oxidized, or removed by mutation of ligands, was ~ 60 – 80 mV higher than that measured by direct titration. Nevertheless, in kinetic experiments, heme b_H becomes reduced before b_L , and the E_m values appropriate to the metastable state after flash activation are the ones measured by redox titration.

- (ii) Equilibration between the oxidized RC and the high potential chain occurs rapidly, but the apparent equilibrium constant is considerably lower than that expected from the E_m values.³⁵ Two mechanisms have been proposed, one based on supercomplexes (^{35–38}), and the other on a heterogeneity in distribution of the components of the photosynthetic chain in the chromatophore vesicles.³⁹ Supporting evidence for supercomplexes is weak,^{40–43} but the explanation in terms of heterogeneity seems to work quite naturally. The theoretical fits to the data depend on assumptions about the size of chromatophores and the stochastic distribution. The distribution function becomes much coarser for smaller numbers of entities per vesicle, and is therefore dependent on whether or not complexes are in dimeric association. Using the fact that both RC/LH1^{38, 41, 42} and bc_1 complexes⁴⁴ are now known to be dimeric, application of the simple algorithm previously suggested³⁹ gives a quantitative fit to the data.

A second important conclusion, implicit in the equilibrium treatment, is that the partial processes are reversible in the ms range; recent attention has been drawn to this feature by Osyczka *et al.*,³² and will be discussed in detail below.

A third conclusion from this treatment is also important. The bifurcated oxidation of QH_2 separates the two electrons, delivering one to the high potential chain of ISP, cyt c_1 and cyt c_2 , and the other to the low potential b -heme chain. The high and low potential chains come rapidly to their own internal equilibria, and the two are in equilibrium, through the Q_o site, with the Q pool. However, the two chains do not otherwise exchange electrons in the ms range. This means that there are, on the timescale of normal turnover, no rapid bypass or short-circuit processes to lower the efficiency of the bifurcation or of the proton-pumping reactions that depend on it. Indeed, under static head conditions, the same equilibrium constants, modified only by the electrical backpressure along the low potential chain, were shown also to account for the redox poise of the photosynthetic chain.^{45, 46} However, although the bifurcated reaction occurs with high efficiency, bypass or short-circuit reactions representing 1–3% of the maximal rate can be readily demonstrated in the presence of inhibitors.^{47, 48} These are thought to involve the semiquinone intermediate formed at the Q_o site.^{49–51}

Several recent publications have aimed to address the complexity of the bc_1 complex,^{32, 52–55} in some cases by simplifying assumptions about the mechanism of the Q_o site. As noted above, Osyczka *et al.*³² extended the equilibrium approach to show that the values for equilibrium constants calculated from redox measurements still

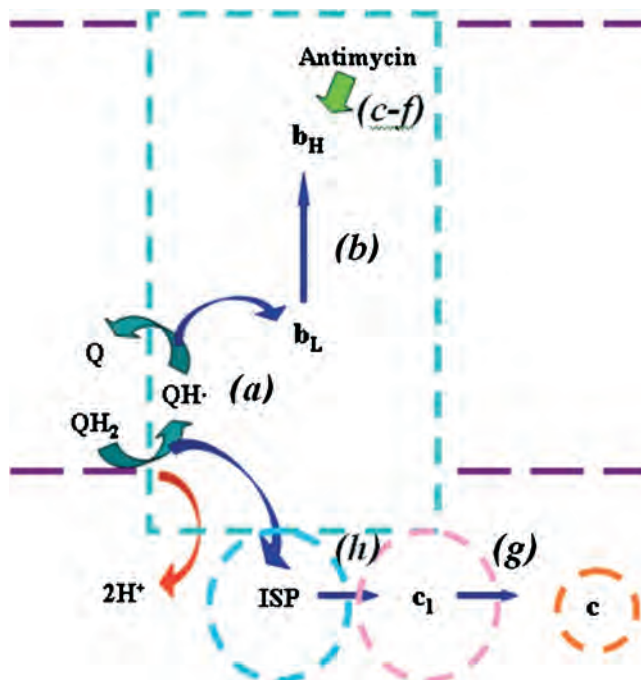


Figure 2 The partial reactions of the Q -cycle in the presence of antimycin. By limiting the turnover at the Q_i site by the inhibitor antimycin, the reactions are constrained to the simpler scheme shown here, involving only the turnover of the Q_o site. The letters identify reactions shown in Table 1

explained the distribution of electrons in chains truncated by mutagenesis. They emphasized the reversibility of the bifurcated reaction in the ms range, and discussed implications for mechanism in the context of rate constants expected from distances revealed by structures. They identified difficulties arising from attempts to account for forward, reverse, and bypass rates at calculated occupancies of the intermediate SQ, which has a putative role of in all these processes. To overcome these, they proposed a bold hypothesis that rejected all mechanisms involving SQ intermediates, and replaced them with two possibilities, a genuinely ‘concerted’ mechanism or a double-gated sequential mechanism in which SQ formed would be immediately consumed. However, in simplifying the problem, they overlooked complexities that allow alternative explanations. I will demonstrate that both of their mechanisms have problematic aspects, but that one of the rejected mechanisms involving a weakly populated SQ intermediate,^{17, 52, 53, 56, 57} can account quite naturally for the experimental observations. A recent review by Rich⁵⁴ has a useful discussion of mechanism using a simple treatment through rate and equilibrium constants based on redox properties of the $Q/SQ/QH_2$ system, following earlier treatments involving an unstable SQ intermediate.^{17, 54, 58} The reaction pathway discussed is similar to that previously proposed,⁵⁶ but the discussion also ignores complexities.

2 Control of Turnover by the Bifurcated Reaction at the Q_o Site

Oxidation of QH₂ at the Q_o site is the rate-limiting step, and tight control of the bifurcation of electrons is essential. With additional physicochemical data, and the availability of structures from crystallography starting about seven years ago,^{5-7, 11, 13, 44, 55, 59-65} we now have important information that has allowed a deeper exploration of this central catalytic function. Several key features from structural analysis bear on the question of how the bifurcated reaction is controlled:

- (i) The modified Q cycle maps naturally onto the structures.
- (ii) The Q_o site can be identified as the binding site for two main classes of inhibitors:
 - (a) Those forming H-bonds to His-161 of ISP. They include stigmatellin, HHDBT, UHDBT, NQNO, and atovaquone (model structure). These necessarily occupy the domain of the Q_o site near the *b*-interface, distal from heme b_L (distal domain). Biophysical evidence has shown that the reduced ISP (ISPH), in which His-161 is protonated, is the active form. The >C=O group of stigmatellin,⁶ or a >C-O⁻ group of HHDBT,⁶² serves as H-bond *acceptor* from the imidazole >N_εH of the *reduced* ISP. Stigmatellin is additionally H-bonded by Glu-272 (chicken numbering) from cyt *b*, with an -OH (across the chromone ring from the H-bond with His-161) acting as H-bond donor.⁵⁶
 - (b) Inhibitors binding in the domain proximal to heme b_L, and forming H-bonds with the peptide -NH of Glu-272.⁵⁷ These include myxothiazol, azoxystrobin, famoxazone, MOA-stilbene and related MOA inhibitors. With the exception of famoxazone,⁶⁵ all structures containing these inhibitors show the ISP displaced towards the *c*-interface.
- (iii) The Q_i-site is identified through occupancy by inhibitors (antimycin, NQNO), or quinone. The binding pocket allows van der Waals contact with the heme b_H edge, and H-bonding of quinone or SQ that may be through sidechains (Asn-221, His-217, Asp-252 in *Rb. sphaeroides*) or water.^{61,66-68}
- (iv) Structures showing cyt *c* at a binding interface on cyt c₁ confirm the location of the third catalytic interface.^{9,69,70}
- (v) The extrinsic domain of the iron-sulfur subunit (ISP) is found in several different positions in different structures (at least eight to date). Berry and colleagues^{6,71,72} suggested that the domain must act as a mobile shuttle of reducing equivalents between the Q_o site and cyt c₁. This conclusion has been amply supported by biophysical, biochemical and molecular engineering studies⁷³⁻⁸⁰. The two interfaces for electron transfer are:
 - (a) A concave external surface of cyt *b* (the *b*-interface) from which an access port allows N_ε of His-161 of ISP (beef numbering) to form H-bonds with certain occupants (inhibitors,⁶ and likely also Q and QH₂^{56, 67, 81-84}) of the Q_o site. His-161 is one of the ligands to the [2Fe-2S] cluster.
 - (b) The *c*-interface on cyt c₁, at which N_ε of His-161 forms an H-bond bridge to a heme c₁ propionate, with a distance appropriate for rapid electron transfer.⁷

- (vi) Mutations giving rise to resistance to inhibitors for the most part map to the internal surfaces of the two inhibitor-binding domains.^{11, 57, 69}
- (vii) In the Q_o site, mutations giving rise to myxothiazol resistance also give rise, in the absence of inhibitor, to a slowing of electron transfer to the *b*-heme chain, suggesting that these mutations block occupancy of this proximal domain by some quinone species during the catalytic cycle, and thus inhibit turnover.⁵⁷
- (viii) None of the structures has shown any well-defined quinone occupant for the Q_o site. However, a recently deposited data set (PDB ID 1ntz) included coordinates for ubiquinone, albeit with B-factors that indicate a rather weak degree of confidence in assignment of electron density. The quinone was in the distal domain, but the distance from the quinone $>C=O$ to N_ϵ of His-161 (4.54 Å) was greater than expected for the H-bond suggested from EPR-studies.⁶⁷

3 The ES Complex

The structural features summarized above have opened a flood of new experimentation, discussion, and speculation about mechanism, much of it reviewed earlier.^{8, 10–12, 14, 52, 64, 69, 75} Rather than repeat this discussion, I will focus on aspects that remain controversial. Perhaps most pertinent to the present discussion is the suggestion that the ES complex, from which electron transfer proceeds, is formed at the distal end of the Q_o site, with the QH_2 forming two H-bonds. In one of these, $-OH$ is a *donor* to the dissociated N_ϵ of His-161 from the *oxidized* ISP (ISP_{ox}), and in the other $-OH$ is a donor to Glu-272 of *cyt b*.^{53, 56, 85} A quinol can be modeled in place of stigmatellin without significant distortion of the structure, to provide distances appropriate to these H-bonds.^{55, 56} Independent evidence in support of such a configuration comes from kinetic measurements to assay the binding forces involved in formation of the ES complex, and changes in these values found in mutant strains.^{56, 86} The main enthalpic contributions are likely to come from the H-bonds above. Since QH_2 and His-161 of ISP form a mutual H-bond, it might be expected from simple mass-action considerations that formation of the ES complex would pull QH_2 ‘out of solution’ in the lipid phase, and the dissociated active form of ISP_{ox} ‘out of solution’ from the mixed states of occupancy of the extrinsic domain in the P phase. Two effects quantified in a number of different labs can be associated with this mutual binding (reviewed in⁵³). These are an apparent shift in the E_m of the Q/QH_2 couple involved in formation of the ES complex, and an apparent shift in the pK of ISP_{ox} , both assayed kinetically through [ES], measured by the rate of reduction of heme b_H in the presence of antimycin. These two displacements show similar driving forces.^{53, 85}

The configuration of the ES complex suggested has important mechanistic implications. Indeed, the success with which the kinetic properties can be accounted for in terms of this starting configuration could be taken as additional justification for its validity. This configuration is shown in Figure 3 (top). The model provides a starting point for discussion of mechanism. Most importantly, because of the structural context, the discussion can be framed in light of the dependence of rate constant on distance demonstrated by Dutton’s group.^{87–90} In order to bring out the utility of this

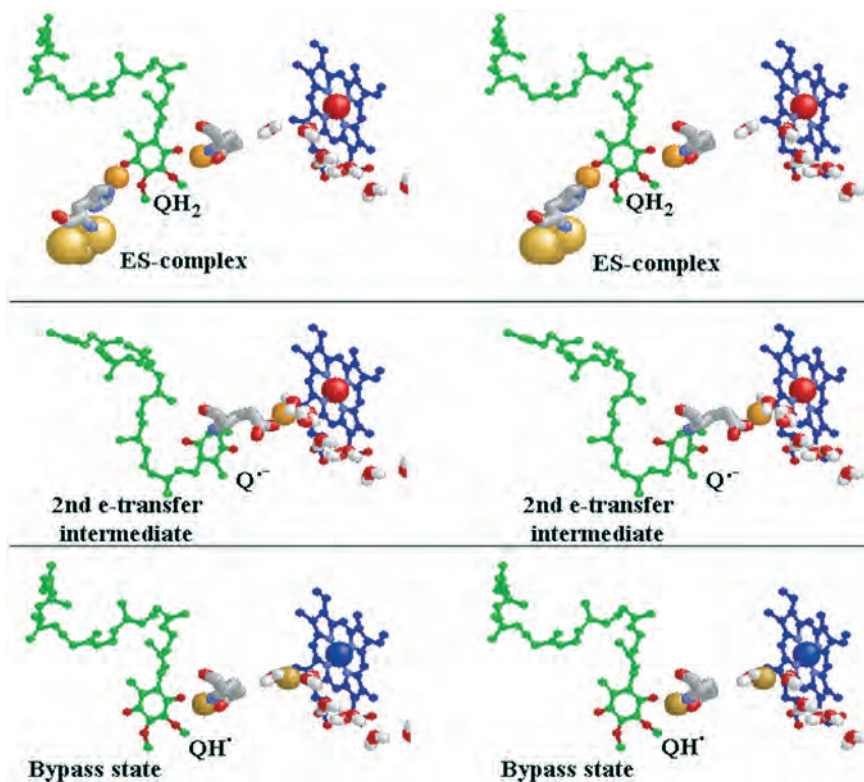


Figure 3 Different states of occupancy of the Q_o site by ubiquinol and semiquinone. Top. The ES complex. The structure of the chicken complex in the presence of stigmatellin (from 2bcc) was modified as follows: the stigmatellin coordinates were stripped from the file. A ubiquinol molecule (ball-and-stick model with C-atoms in green) was then docked in the Q_o site as described in ref.⁵⁶ The model was allowed to relax with constraints on the position of ubiquinol through tethers to the two proposed ligands, to remove van der Waals clashes, followed by relaxation without constraints. Ligands are shown as tube models, with His-161 of ISP on the left, and Glu-272 of cyt *b* on the right. Heme b_L is shown as a ball-and-stick model, with C-atoms in blue. In all models, the protons associated with the mechanism of QH_2 oxidation are shown as van der Waals radius spheres, colored orange. Middle. The state from which the second electron transfer occurs. Heme b_L is oxidized (Fe colored red), and the $Q^{\cdot-}$ intermediate can access the proximal domain. For this model, the quinone was relaxed in the context of a structure from which the myxothiazol occupant was replaced. Bottom. The bypass state. When heme b_L is reduced (Fe colored blue), oxidation of SQ cannot occur, and coulombic repulsion prevents formation of $Q^{\cdot-}$ and coulombic attraction discourages H^+ exit down the water chain. Both effects contribute to keeping QH in the distal domain. The strong positive ΔG^0 keeps the occupancy of SQ at $< 10^{-6}$. Stereo pairs for crossed-eye viewing

approach, note that electron transfer events in the pseudo-solid-state of the protein interior are first order, with rates dependent on fractional occupancy:

$$v = k_{\text{cat}}[\text{occupancy}] \quad (1)$$

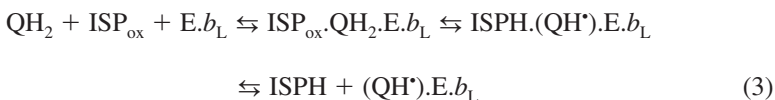
This relationship is familiar from classical enzyme kinetics, where the fractional occupancy of the ES complex is assayed through the steady-state rate. The term [occupancy] here refers to the fraction of centers in the state from which reaction proceeds; for redox reactions, this will be determined by the product of donor and acceptor occupancies. In light of the above relationship, a distance from the structure can provide constraints, either if ν or [occupancy] is known. A value for $\log_{10}k_0$ is calculated from the distance, R (see Equation 2), using the first two terms from the Moser–Dutton equation (with $\beta = 1.4$), and k_{cat} can then be estimated if appropriate values are available for the other parameters, ΔG^0 (standard free-energy change for the reaction, or driving force), and λ (Marcus reorganization energy), included in the right-hand term.

$$\log_{10} k_{\text{cat}} = 13 - \frac{\beta}{2.303}(R - 3.6) - \gamma \frac{(\Delta G^0 + \lambda)^2}{\lambda} \quad (2)$$

The latter values are related to the activation energy through the Marcus expression, $\Delta G^\ddagger = (\Delta G^0 + \lambda)^2/4\lambda$, suggesting several experimental routes for determination. Note that Equation 2 is an expanded form of the Arrhenius equation in \log_{10} form, with the right-hand term replacing the Arrhenius activation barrier. The factor γ is either $(F/(4 \times 2.303 RT)) \sim 4.23$ at 298 K) in the classical Marcus treatment,^{91, 92} or a similar term modified by quantum mechanical contributions due to tunneling, with a value of 3.1 in the Moser–Dutton treatment. The Marcus value gives lower rate constants than the Moser–Dutton term, especially for high values of λ . The Arrhenius equation and its various derivatives also provide constraints on rate. Under conditions of substrate saturation, $k_{\text{cat}} = k_0 \exp\{-\Delta G^\ddagger/RT\} \approx k_0[\text{ES}^\ddagger]$. This is because, in the standard treatment, $-\Delta G^\ddagger/RT = \ln K^\ddagger$, and $K^\ddagger = [\text{ES}^\ddagger]/[\text{ES}]$, so that $[\text{ES}^\ddagger]$ becomes equal to the fractional occupancy of the activated state if $[\text{ES}^\ddagger] \ll [\text{E}_{\text{tot}}]$.

4 Constraints from the ES-complex Model

Rate constants and activation barriers measured for the partial processes are shown in Table 1. In discussion of their results, Hong *et al.*⁹³ assumed that the bifurcated reaction occurred through two separate one-electron transfer reactions, with a finite, though low, occupancy of the intermediate bound SQ state (QH[•]).E.b_L.



This assumption was based on a number of observations. A dependence of rate on driving force is predicted from the Marcus relationship. Although the E_{m} values of the SQ couples involved are unknown, on the assumption that these do not change, the driving forces for the two one-electron steps could be varied through changes in E_{m} values for their electron acceptors. The dependence of rate on the E_{m} of ISP, the acceptor in the high potential chain, has been studied in several labs through use of

ISP mutant strains with modified E_m .^{53,82,86,94,95} The results showed that the rate of the overall reaction decreases with lowered driving force, as expected from Marcus theory if the first electron transfer is limiting. A remarkable uniformity in behavior across the bacterial–mitochondrial divide, and among different bacteria, provides a high level of confidence that the results are not due simply to non-specific effects. In contrast, no simple Marcus behavior has been reported on modification of the E_m of heme b_L , the acceptor in the low potential chain.⁹³ In all reported cases, the rate was lowered or unaffected when the E_m of heme b_L was raised by mutation. From this, it seems reasonable to conclude that transfer of the first electron from QH₂ to ISP determines the overall rate of the bifurcated reaction. In this sequential mechanism, SQ is an intermediate product, removed on transfer of the second electron to heme b_L .

An important lesson from these results is that they are in contradiction with any genuinely ‘concerted’ reaction.^{53,93} The two electron transfers to two distinct chains would have to occur from a common activated state with the same intrinsic rate constant and other Marcus parameters. If such a reaction did occur, both steps would be under the same constraint of driving force, and, apparently, they are not.

The alternative is some sort of sequential mechanism. What constraints are provided by the two hypotheses above, that the first electron transfer is rate limiting, and that the ES complex has the structural configuration proposed? A consequence of these two hypotheses is that the first (limiting) electron transfer occurs through the ~7 Å distance from the O atom of the quinol –OH to the nearest Fe atom of the cluster. The distance is bridged by the H-bond to His-161 and the histidine ring, providing a plausible through-bond path of this distance. With values for the Moser–Dutton variables in conventional ranges ($\beta \sim 1.4$, $\lambda \sim 0.7$ V, $\gamma = 3.1$), the expected rate constant would be in the sub- μ s range. Even with the endergonic ΔG^0 appropriate for an unstable SQ, the expected rate is at least three orders of magnitude faster than measured. The problem is therefore how to explain the slow rate observed. The rate can be accounted for only if a value for $\lambda > 2.0$ V is used. This is consistent with the high activation barrier for the overall reaction ($\Delta G^\ddagger \sim 550$ – 650 mV), supporting the hypothesis that this barrier is in the first electron transfer.^{17,93} However, this is not altogether satisfactory, because there are no obvious features of the structure that might explain the high value for reorganization energy, λ , and the linked high ΔG^\ddagger .

5 Proton-coupled Electron Transfer

In order to proceed further, we now have to consider several complicating factors. The first of these is the involvement of a proton in the first electron transfer. In order to form the proposed H-bond, either His-161 of ISP_{ox} or the quinol –OH would have to lose a proton. It now seems well established that the pK of 7.6 on ISP_{ox} is due to dissociation of one of the histidine ligands to the cluster, likely His-161.^{96–99} If so, the probabilities for dissociation are easily calculated from the pK s, and they favor by a factor of ~1000 the dissociation of His-161. However, on reduction, the pK of ISP is shifted from 7.6 to 12.4, and this would lead to uptake of H⁺. At the same time, the pK of the quinol would shift on oxidation from >11.3 to the acid range for QH⁺, favoring release of a H⁺ to yield QH[•]. The net result would be transfer of both the electron and a proton to ISP. What does this entail mechanistically? If the configuration of the

protein interface in the ES-complex state is similar to that in the stigmatellin complex, then the interface around the H-bond is anhydrous and apolar; there are no groups immediately available for proton exchange. The electron and the proton must therefore both be transferred across the H-bond joining the two groups. Similar reactions in chemistry are discussed as proton-coupled electron transfer reactions.^{100, 101} We then have two obvious possibilities for the sequence of the partial processes: electron first or proton first.^{85, 99} Since the proton transfer probability is determined by the pK s of donor and acceptor groups (QH_2 , ISP_{ox}) through a Brønsted relationship, the different probabilities can be calculated from the pK s using a thermodynamic square and the overall free-energy change.⁸⁵ For the endergonic first electron transfer expected, transfer of the proton first is strongly favored, despite the fact that this step is itself endergonic ($\Delta G^0 = 2.303RT(pK_D - pK_A) > 21\text{--}27 \text{ kJ mol}^{-1}$, depending on choice of bound or free pK values for ISP_{ox}). The slow rate can then be readily explained by the fact that electron transfer occurs from this weakly occupied intermediate state. The electron transfer rate constant, k_{ET} , has the value expected from the distance and a conventional value for λ , but the observed rate constant, given by $k_{app} = k_{ET}K_{proton}$, where K_{proton} is between 10^{-4} and 10^{-6} , is lowered by the weak occupancy. The first electron transfer can now be dissected into the partial processes shown in Figure 4, with approximate $\Delta G^{0'}$ values (in electrical units), and rate constants, as shown in the legend. Expanding the relationship for k_{app} into the Moser–Dutton equation gives:

$$\log_{10} k_{app} = 13 - \frac{\beta}{2.303}(R - 3.6) - \gamma \frac{(\Delta G_{ET}^0 + \lambda)^2}{\lambda} - (pK_D - pK_A)$$

In addition to explaining the paradoxical properties of the first electron transfer, this equation also accounts for the previously unexplained kinetic behavior of an ISP mutant strain in which the pK was changed from 7.6 to 8.5.^{53, 86}

A third possibility for the sequence of partial processes is simultaneous transfer of H^+ and e^- , essentially along the diagonal of the thermodynamic square.^{99, 100} Although not excluded, such mechanisms have the disadvantage that the diagonal pathway would necessarily be of lower energy than the alternatives, removing the explanation for the slow rate provided by the proton-first mechanism.

6 The Second Electron Transfer, From SQ to Heme b_L

Consideration of the second electron transfer brings up another complicating factor. Attempts to measure the intermediate SQ state through EPR have failed to detect any species with the expected properties.^{17, 58} It might be argued that this is not surprising. In order to reduce heme b_L , the Q/SQ couple would have to have an $E_m < -90 \text{ mV}$. Substitution of values in this range into the standard equations (using an E_m of 90 mV for the quinone pool), give values for the SQ/ QH_2 couple appropriate for reduction of ISP at an E_m of 300. A stability constant for the disproportionation reaction, $K_S \leq 10^{-6}$, can be calculated from these E_m values, giving an equilibrium occupancy in the range of $10^{-4} - 10^{-3} \text{ monomer}^{-1}$, which would be undetectable. Osyczka *et al*³² discussed the mechanistic occupancy at the Q_o site in terms of K_S . However, the stability constant is clearly not appropriate for calculation of mechanistic occupancies. The reaction

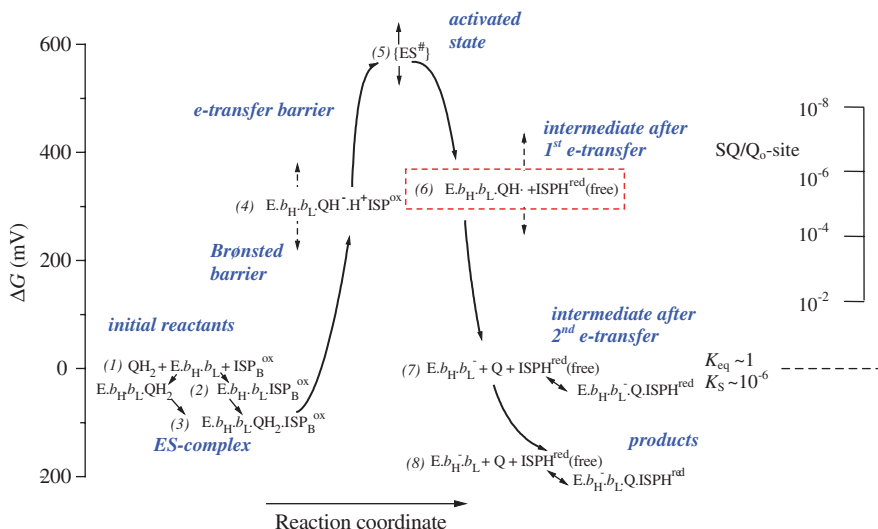


Figure 4 An energy landscape for the Q_o -site reactions. In order to keep track of the thermodynamic interplay in this complex set of reactions, a computer program to model the Q_o -site reactions was written that balances the terms within appropriate physicochemical constraints, and allows the user to explore how each of the parameters discussed in the text effects the rate. Variables include driving forces for both electron transfer steps, relative binding constants for Q and QH_2 , stability of the SQ , λ for each electron transfer reaction, contributions of the Brønsted term, distances, activation barriers, pK values, etc. The Visual Basic program in executable and source form is available for downloading.¹²⁵ The data are presented as free-energy differences, but it should be obvious that conventional conversions allow alternative presentation in terms of equilibrium constants and rate constant, using the data from Table 1 and below. The inserted scale to the right shows occupancies for the SQ state, based on equilibrium constants for the one-electron transfer reactions, in units of $[SQ] [bc_1 \text{ monomer}]^{-1}$. Partial reactions for the first electron transfer are:

Reaction	Process	$\Delta G^{0'}$	k_{forward}	k_{reverse}
$QH_2 + ISP_{\text{ox}} + E.b_L \rightleftharpoons ISP_{\text{ox}}.QH_2.E.b_L$	(1–3)	-80*	$1.4 \times 10^5 \text{ M}^{-1}\text{s}^{-1}$	$\sim 10^4 \text{ s}^{-1}$
$ISP_{\text{ox}}.QH_2.E.b_L \rightleftharpoons ISPH^+.QH^-.E.b_L$	(4)	360	10^5 s^{-1}	10^{11} s^{-1}
$ISPH^+.QH^-.E.b_L \rightleftharpoons \{ISPH^+QH^-\}^#.E.b_L$	(5)	300	10^6 s^{-1}	10^{11} s^{-1}
$\{ISPH^+QH^-\}^#.E.b_L \rightleftharpoons ISPH + (QH^).E.b_L$	(6)	-300	10^{11} s^{-1}	10^6 s^{-1}
$QH_2 + ISP_{\text{ox}} + E.b_L \rightleftharpoons ISPH + (QH^).E.b_L$ (1st e ⁻)		280	$1.3 \times 10^3 \text{ s}^{-1}$	$6 \times 10^7 \text{ s}^{-1}$

In these equations heme b_H has been omitted for clarity, $ISP_{\text{ox}}.QH_2.E.b_L$ is the ES-complex, and $\{ISPH^+QH^-\}^#.E.b_L$ is $\{ES^\#\}$ in the Figure. Equation identifiers refer to numbers in the Figure. Values are approximate within the ranges shown by arrows on the scheme (see ⁹³ for details).

*Note. The value in electrical units is derived from apparent binding constants and is not normalized to concentration.⁵³

under consideration is not the equilibrium disproportionation of Q and QH₂, but the bifurcated electron transfer to two separate acceptors. This does not occur at redox equilibrium, but only under the metastable conditions in which the quinone pool is reduced and ISP oxidized. For the sequence of reactions shown by Equations 3 and 4, the equilibrium constants could in principle be calculated separately, but with the constraint that $K_{\text{eq}}^3, K_{\text{eq}}^4 = K_{\text{Q0}}$, the equilibrium constant for the bifurcated reaction. The value for K_{Q0} is between 1 and 20 (depending on species, and choice between bound and free Q/QH₂). If the E_{m} values were as above, K_{eq} would be ~ 1 for each process in *Rb. sphaeroides*, and a SQ occupancy of $\sim 0.33 \text{ monomer}^{-1}$ would be expected, well within the range of detectability.

Nevertheless, a much lower occupancy is expected for a different reason. The bc_1 complex, when operating in the presence of antimycin, or under other conditions (high proton motive force, mutation in the Q_i site) leading to an inhibition of flux out of the Q₀ site, generates superoxide, a precursor to the reactive oxygen species that lead to DNA damage and cellular aging.^{48, 49} The reductant for O₂ is thought to be the SQ generated at the Q₀ site.⁴⁹ In order to minimize this deleterious reaction, it is likely that evolution has designed the site to keep the SQ at as low a concentration as possible compatible with rapid forward electron transfer, and to insulate it from reaction with O₂.⁵⁷

7 Kinetic Estimation of SQ Occupancy

In order to find limiting values for the lowest kinetically compatible SQ occupancy, Hong *et al.*⁹³ explored a range of scenarios for the second electron transfer, based on use of Equation 1 in consideration of the parameters noted above, the constraints on rate constant from distances shown by the structures, and the occupancy. They considered three possibilities:

- (i) That the SQ remained in the location at the distal end of the site where it was formed.
- (ii) That the SQ could move from this site to the proximal domain close to heme b_L .
- (iii) That a second quinone could bind in the domain proximal to heme b_L and facilitate electron transfer between the Q/SQ generated in the distal domain and heme b_L .

The reaction configuration summarized under (i) would strongly constrain the kinetic values because of the long distance for transfer of the second electron from SQ to heme b_L . For example, with $\lambda = 0.75 \text{ V}$, $\Delta G^o = -.38 \text{ V}$, and a distance of 12.4 \AA , k_{cat} is $\sim 1.22 \times 10^7 \text{ s}^{-1}$. As a consequence, any SQ occupancy lower than $\sim 10^{-4}$ would give a rate lower than that measured, and was therefore considered to be unrealistic in this scenario.

Mechanisms in which the intermediate state is constrained to the distal domain include variants of that proposed by Link,¹⁰² and discussed by Hong *et al.*⁹³ Berry and Huang⁵⁵ have also discussed a version of this mechanism, in which the $\text{ISP}_{\text{ox}}\cdot\text{QH}_2 \rightleftharpoons \text{ISPH}\cdot\text{QH}\cdot$ equilibrium mix acts as the electron transfer state from which heme b_L is

reduced. The fractional occupancy of the right-hand state would be the critical term, and could be determined by an equilibrium constant higher than allowed in models in which dissociation occurs. Kinetic measurements provide constraints on the highest possible occupancy of intermediate states.⁵² The $\sim 120 \mu\text{s}$ lag in reduction of heme b_{H} following flash activation of turn-over in *Rb. sphaeroides* chromatophores must be accounted for in terms of all delays in delivery of substrates to the Q_o site following the flash. With the quinone pool partly reduced, these delays are in the high-potential chain, and in the population of intermediate states in the bifurcated reaction. If, as we have demonstrated, the intermediate SQ state is after the activation barrier, it must be formed at the limiting rate. Since lags in the high potential chain account for $\sim 100 \mu\text{s}$, maximal occupancy is given approximately by (unaccounted lag)/(limiting lifetime), or $20/770 \sim 0.025$ (lag and lifetime values are in μs). Thus, mechanisms in this class are constrained to occupancies between $\sim 10^{-2}$ and 10^{-4} SQ/monomer.

7.1 Estimation of SQ Occupancy from Bypass Rates

From the importance of occupancy of SQ in this discussion, it is clear that an alternative method for estimation of this value would be useful. A number of potential bypass (or short-circuit) reactions have been previously discussed, all of which involve SQ as donor or acceptor of electrons.⁵¹ In view of this, Osyczka *et al.*³² suggested an approach based on the rate of these reactions. The general idea follows the method already discussed in⁹³ and above. Using Equation 1, occupancy can be calculated from a rate constant estimated from the structures, and from the measured short-circuit rate. The four pathways discussed are shown in Table 2. In estimation of rate constants, Osyczka *et al.*³² assumed that the SQ was positioned in the domain occupied by stigmatellin (the distal domain), and that the appropriate distances were either 6.8 \AA to ISP for oxidation of SQ, or 12.4 \AA for reduction by heme b_{L}^- . The first reaction discussed was the reduction of ISP_{ox} by the SQ formed after the first electron transfer (Table 2 (a)). From the limited information presented, it seems likely that they used a distance of $\sim 7 \text{ \AA}$, a value for $\lambda \sim 1.0 \text{ V}$, and an assumed $\Delta G^{0'} \sim 0$, to give $k \sim 7 \times 10^7 \text{ s}^{-1}$. Using the rate they measured (0.3 s^{-1}), this gives a SQ occupancy of $\sim 4 \times 10^{-9} \text{ monomer}^{-1}$, from which $K_{\text{S}} \sim 10^{-16}$, the value they gave. However, as noted above, the equilibrium constant, K_{S} , although a convenient shorthand for the E_{m} values of the one electron couples, is not related to the actual equilibrium constant for the electron transfer reactions, and its use could be misleading. A second complication is that the short-circuit rates they measured were an order of magnitude slower than those reported in the literature (*cf.*^{48, 51} and see Table 3). Using a more realistic rate of 3 s^{-1} , and otherwise similar assumptions, occupancy would be $\sim 4 \times 10^{-8} \text{ monomer}^{-1}$. Thirdly, the reaction equations all involve electron transfer between donor and acceptor pairs; the calculated occupancy of SQ would have to be greater if the occupancy of its reaction partner were < 1 . With these caveats, we can use the occupancy of SQ and the arguments above to calculate a rate for the second electron transfer required for QH₂ oxidation. The rate using a rate constant of $\sim 1.22 \times 10^7 \text{ s}^{-1}$ (calculated as above) is then incompatible with the observed overall rate of turnover; the maximal rate would be $< 1 \text{ s}^{-1}$ instead of $1.3 \times 10^3 \text{ s}^{-1}$. In light of the argument leading to this rate constant, and as previously

Table 2 Reactions proposed for bypass or short-circuit of the bifurcated reaction

Partial reactions leading to bypass	Occupancy	k_{max} or (k_{dist})	Rate (s^{-1})	ID and refs.
$\text{QH}_2 + \text{ISP}_{\text{ox}} + \text{E}.b_{\text{L}}^- \rightleftharpoons \text{ISPH} + (\text{QH}^*)\text{E}.b_{\text{L}}^-$ $\text{ISPH} + \text{cyt } c_2^+ \rightleftharpoons \text{ISP}_{\text{ox}} + \text{cyt } c_2 + \text{H}^+$ $(\text{QH}^*)\text{E}.b_{\text{L}}^- + \text{ISP}_{\text{ox}} \rightleftharpoons \text{Q} + \text{E}.b_{\text{L}}^- + \text{ISPH}$ $\text{ISPH} + \text{cyt } c_2^+ \rightleftharpoons \text{ISP}_{\text{ox}} + \text{cyt } c_2 + \text{H}^+$	4×10^{-8}	7×10^7	2.8	(a) {c} 32, 51
$\text{QH}_2 + \text{ISP}_{\text{ox}} + \text{E}.b_{\text{L}}^- \rightleftharpoons \text{ISPH} + (\text{QH}^*)\text{E}.b_{\text{L}}^-$ $\text{ISPH} + \text{cyt } c_2^+ \rightleftharpoons \text{ISP}_{\text{ox}} + \text{cyt } c_2 + \text{H}^+$ $(\text{QH}^*)\text{E}.b_{\text{L}}^- + \text{O}_2 \rightleftharpoons \text{Q} + \text{E}.b_{\text{L}}^- + \text{O}_2^-$ $\text{O}_2^- + \text{cyt } c_2^+ \rightleftharpoons \text{O}_2 + \text{cyt } c_2 + \text{H}^+$	4×10^{-8}	7×10^7	2.8	(a') 32, 45, 51
$\text{E}.b_{\text{L}}^-b_{\text{H}}^- + \text{Q} + \text{H}^+ \rightleftharpoons (\text{QH}^*)\text{E}.b_{\text{L}}^-b_{\text{H}}^-$ $(\text{QH}^*)\text{E}.b_{\text{L}}^-b_{\text{H}}^- \rightleftharpoons (\text{QH}^*)\text{E}.b_{\text{L}}^-b_{\text{H}}^-$ $(\text{QH}^*)\text{E}.b_{\text{L}}^-b_{\text{H}}^- + \text{H}^+ \rightleftharpoons \text{QH}_2 + \text{E}.b_{\text{L}}^-b_{\text{H}}^-$ $\text{QH}_2 + \text{E}.b_{\text{L}}^-b_{\text{H}}^- + \text{cyt } c_2^+ \rightleftharpoons \text{Q} + \text{E}.b_{\text{L}}^-b_{\text{H}}^- + \text{cyt } c_2 + 2\text{H}^+$ $\text{QH}_2 + \text{E}.b_{\text{L}}^-b_{\text{H}}^- + \text{cyt } c_2^+ \rightleftharpoons \text{Q} + \text{E}.b_{\text{L}}^-b_{\text{H}}^- + \text{cyt } c_2 + 2\text{H}^+$	0.2 4×10^{-11}	1.2×10^3 $< 1 \times 10^{11}$	240 < 4	(b) {d} 32
$\text{QH}_2 + \text{ISP}_{\text{ox}} + \text{E}.b_{\text{L}}^- \rightleftharpoons \text{ISPH} + (\text{QH}^*)\text{E}.b_{\text{L}}^-$ $(\text{QH}^*)\text{E}.b_{\text{L}}^- + \text{H}^+ \rightleftharpoons \text{QH}_2 + \text{E}.b_{\text{L}}^-$	4×10^{-8}	1×10^{11} or	4000 or	(c) {e}
$\text{QH}_2 + \text{ISP}_{\text{ox}} + \text{E}.b_{\text{L}}^- \rightleftharpoons \text{Q} + \text{ISPH} + \text{E}.b_{\text{L}}^- + \text{H}^+$ $2(\text{ISPH} + \text{cyt } c_2^+ \rightleftharpoons \text{ISP}_{\text{ox}} + \text{cyt } c_2 + \text{H}^+)$	4×10^{-8}	(5×10^7)	2	32, 45, 51
$\text{E}.b_{\text{L}}^-b_{\text{H}}^- + \text{Q} + \text{H}^+ \rightleftharpoons (\text{QH}^*)\text{E}.b_{\text{L}}^-b_{\text{H}}^-$ $(\text{QH}^*)\text{E}.b_{\text{L}}^-b_{\text{H}}^- + \text{ISP}_{\text{ox}} \rightleftharpoons \text{Q} + \text{E}.b_{\text{L}}^-b_{\text{H}}^- + \text{ISPH}$ $\text{ISPH} + \text{cyt } c_2^+ \rightleftharpoons \text{ISP}_{\text{ox}} + \text{cyt } c_2 + \text{H}^+$ $\text{QH}_2 + \text{E}.b_{\text{L}}^-b_{\text{H}}^- + \text{cyt } c_2^+ \rightleftharpoons \text{Q} + \text{E}.b_{\text{L}}^-b_{\text{H}}^- + \text{cyt } c_2 + 2\text{H}^+$	0.2 4.10^{-8}	1.2×10^3 7.10^7	240 2.8	(d) {f} 32

Notes:

For each of the above sets of partial processes, the overall reaction is the scalar part of the reaction catalyzed by the uninhibited Q_0 site, $\text{QH}_2 + 2 \text{cyt } c_2^+ \rightleftharpoons \text{Q} + 2 \text{cyt } c_2 + 2\text{H}^+$. The letters in the right-hand column identify either (in parentheses) reactions referred to in the text, or (in curly brackets) the equivalent reaction in Figure. 6 of. ³² Values for occupancy, rate constants and rate are calculated as described in the text.

Table 3 Rates of bypass reactions in wild type and mutant strains

Reaction used to measure bypass	Inhibitor	Bypass Rate($e/bc_1/s$)	QH_2 oxidation(s^{-1})	QH_2 oxidation measured through:	Bypass as % QH_2 oxidation	Ref.
Heme b_L reoxidation at pH 7	H212N (heme b_H removed)	0.32	1200	redn. heme b_H (in WT)	0.026	32
Cyt c reduction, yeast bc_1 complex ^a	antimycin	3.25	160	cyt c redn. with no inhibitor	2.03	51
Flux into high pot. chain, Q-pool red ^b	antimycin, anaerobic	4–8	600	reduction heme b_H	~1.0	45
RC reduction ^c						
WT		1.35	237		0.6	See note ^d
E295W	antimycin, aerobic	1.5	2.0	Reduction of heme b_H with antimycin,	75	
E295L		2.8	7.18	or (RC redn. with no inhibitor)	39	
E295G		1.46	2.7		54	
E295Q		1.76	9.8		18	
E295D		1.56	14 (23)		11 (7)	
E295K		1.25	3.2 (6.7)		39 (19)	

^aThe bypass rate due to O_2^- production was measured as $2.26 s^{-1}$ electrons/ Q_b site; that due to reduction of semiquinone by heme b_L was $0.99 s^{-1}$.

^bMyxothiazol sensitive, antimycin insensitive rate of RC reduction, anaerobic conditions, E_h , 120 mV.

^cAerobic conditions with 1 mM Na-ascorbate added as reductant (~1 QH_2/bc_1), 2 mM KCN to block oxidases.

^dLee, S., Crofts, S.B., Li, J.-Y., Rose, S. and Crofts, A.R., in preparation.

noted,⁹³ we can effectively eliminate from consideration hypotheses in which a reaction intermediate is constrained to the distal domain, and has an occupancy in this range. A similar constraint applies to ‘concerted’ reactions, for which an occupancy for $[ES^\#] \sim 10^{-10} \text{ monomer}^{-1}$ is determined by $\Delta G^\#$.

Osyczka *et al.*³² framed their main discussion around the lower occupancy they calculated, the difficulties that even this low occupancy gave rise to in understanding how short-circuits are avoided, and how the rapid rate for back reactions needed to explain the reversibility could be accounted for. Indeed, if the rate constant for reduction of Q by heme b_L^- is calculated assuming occupancy of the distal position, and the highly endergonic reaction implied by the value of $E_m \text{ Q/SQ}$ derived by calculation from their K_S value, the back-reaction rates would certainly be much too slow to explain reversibility. However, Berry and Huang⁵⁵ made the interesting point that their equilibrium mix could be a potential substrate for the backreaction from heme b_L^- . The $(\text{ISP}_{\text{ox}}\cdot\text{QH}_2 \rightleftharpoons \text{ISPH}\cdot\text{QH}\cdot)$ state differs from the enzyme-product complex represented by the $g_x = 1.800$ complex (ISPH-Q) by one reducing equivalent. The latter is stabilized in the distal domain by the binding constant involved in its formation, with occupancy ~ 0.5 under physiological conditions.^{31,103,104} Any value for $\Delta G^{0'}$ for formation of $\text{ISPH}\cdot\text{QH}\cdot < 0.3 \text{ V}$ (with $\lambda \sim 0.7 \text{ V}$) would give a rapid enough back reaction. However, since this complex is constrained to the distal domain, the arguments above place limits on the occupancy of this SQ state for viable forward rates.

8 Mobility in the Q_0 site

The second possibility considered by Hong *et al.*⁹³ (ii) above), opens up a wider range of possibilities, but requires particular characteristics of the reaction mechanism. They suggested that, after formation of SQ, the intermediate EP complex dissociates to liberate ISPH and SQ. A mechanism in which ISPH dissociates from the intermediate $\text{ISPH}\cdot\text{SQ}$ complex also seems to be required to account for bypass reactions.^{45,51} Dissociation to liberate SQ in the Q_0 site allows movement close to heme b_L (Figure 3, middle), and this can change the rate constant dramatically. Taking a distance of $< 6.3 \text{ \AA}$ (the distance from myxothiazol to heme b_L), but otherwise the same parameters as above, k_{cat} has a value $> 6.5 \cdot 10^{10} \text{ s}^{-1}$. The calculated rate using the occupancy above is then in the range observed experimentally.

Arguments similar to those developed above can be used in consideration of the back reaction. The electron acceptor from heme b_L^- is Q, which would also likely be mobile in the Q_0 site, and therefore able occupy the proximal domain. Assuming an endergonic $\Delta G^{0'}$ of $< 0.48 \text{ V}$, the reverse rate constant, $k_{-2} \geq 1.2 \times 10^3 \text{ s}^{-1}$, would certainly be adequate to explain reversibility, even with an occupancy of $Q < 1$.

From this discussion, it is clear that the scope for plausible mechanisms is greatly increased by allowing consideration of mobility for SQ and Q in the Q_0 site.

The values used in outlining the arguments above are approximations. In particular, we have used the Moser–Dutton term in all calculations, rather than the classical Marcus term, and contributions of protolytic processes (except for the first electron transfer) have not been separated out. The calculations should therefore be seen as illustrative rather exact. Hong *et al.*⁹³ discussed a wider range of scenarios,

and the limitations on the approximations they used. I will not elaborate further here, except to reiterate that values for K_{eq} for the reactions involving SQ are more appropriately calculated from the E_m of the bound rather than free couples (E_m (Q/QH₂-bound) \sim 130 mV rather than 90 mV for the pool). We have used the same equation for both exergonic and endergonic processes, since, if a value for γ of 4.23 (appropriate to the Marcus treatment) is used, the same result is obtained with equations recommended for exergonic⁸⁸ or endergonic⁹⁰ reactions. However, the endergonic treatment recommended by Page *et al.*⁹⁰ gives a change in slope at the exergonic to endergonic transition, because the quantum mechanical correction leading to $\gamma = 3.1$ is applied to only a part of the endergonic activation barrier (see Appendix 1).

The energy landscape of Figure 4 summarizes the results of an exploration of the Q_o site reactions compatible with low SQ occupancy, using the computer program described in the legend. The free-energy differences between different intermediate states of the bifurcated reaction are shown plotted against an arbitrary reaction coordinate. The dependence of all rates on occupancy, and the interdependence of the bound Q, SQ, QH₂ system parameters, introduce some interesting play-offs between driving force and occupancy that have to be considered in the context of the different choices for distance and standard thermodynamic constraints, as discussed at length by Hong *et al.*⁹³ Since values for several parameters are unknown except within limits, some energy levels are shown by ranges. These represent values that allow forward and reverse rates compatible with the data as summarized in Table 1, assuming the mobility of quinone species in the Q_o site discussed above.

It seems clear from the above that some of the problems hinted at by Osyczka *et al.*³² depend on choice of constraints. If the reactions of the quinone species are all limited by occupancy of the distal domain, rates involving the intermediate SQ state are problematic because of conflicting values needed to match measured rates of forward, reverse and bypass reactions.

9 Other Problematic Short Circuits and Their Prevention

Osyczka *et al.*³² concluded that a value for $K_s < 10^{-16}$ (for bypass reactions (a) and (b), Table 2), or $K_s < 10^{-22}$ (for (c) and (d)) would be required to slow the short-circuits to the seconds range. They provided no detailed justification for these values, but they correspond to SQ occupancies of $< 5 \times 10^{-9}$ and $< 5 \times 10^{-12}$, respectively, and reflect the slow rate of bypass they measured, as discussed above. Because we have used short-circuit (a) as the basis for calculation of SQ occupancy, this provides a reference point rather than a problem. However, using the occupancy of 4×10^{-8} , some of the other short-circuits resulting from reduction of Q or SQ by heme b_L^- ((b)–(d)) do appear to provide difficulties. Two of these, (b) and (d), involve the reduction of Q by heme b_L^- to form SQ. These would occur in competition with the normal reverse reaction. The reaction would occur only under metastable conditions, would be strongly endergonic in the first step, and would lead to a low occupancy of the SQ state. In (b), the second electron transfer through heme b_L^- would occur from a low occupancy of the b_L^- state due to the large equilibrium constant with heme b_H^- . The product of occupancies is in the range

10^{-11} , compensating for even the highest rate constant expected (see below), to give a low net rate. In short-circuit (d), leading to the subsequent oxidation of SQ by ISP_{ox} , the latter rate would be limited by the constraints, already considered above, arising from the low occupancy of the SQ state. Reaction (c) involves the reduction of SQ, generated in the first electron transfer of the forward reaction, by heme b_L^- . This was previously considered by Chen⁴⁵ and by Muller *et al.*⁵¹ as a bypass reaction leading to net oxidation of QH_2 , as shown by the partial reactions in Table 2. The strongly exergonic reduction of SQ by heme b_L^- leads to a calculated rate constant much higher than that for reduction of Q. This would certainly be problematic if the SQ intermediate could be reduced in the proximal domain. For example, with SQ in the proximal domain, a value for $k_{\text{cat}} \sim 1 \times 10^{11}$ is calculated using $\Delta G^{0'} \sim 0.5$ V, and $\lambda \sim .75$ V, and this would allow rates in the 10^3 s^{-1} range even at the low occupancies suggested above. A similar situation would arise on reduction of Q through heme b_L (reaction (b)) if electron transfer between the b_L hemes across the dimer interface could occur. For comparison, the experimental rate, determined from the fraction of bypass that could be attributed to reduction of SQ by heme b_L^- , was about 30% of the total bypass in the presence of antimycin,⁵¹ giving a rate of $\sim 1 \text{ e}^- \text{ monomer}^{-1} \text{ s}^{-1}$. Clearly, the thousand-fold discrepancy between the calculated and observed rates needs to be addressed.

9.1 Double-gating

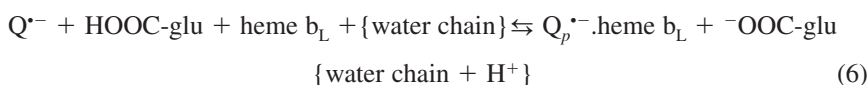
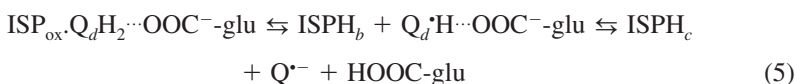
As an alternative to their ‘concerted’ reaction, Osyczka *et al.*³² considered solutions in which the bifurcated reaction operated with a SQ intermediate, but with double-gating to ensure that no reaction generating the SQ could take place unless the complementary reaction removing it also occurred. This would ensure that no build-up of SQ could occur, neatly explaining the low rates for short-circuit reactions they had observed, while allowing a higher occupancy of intermediate states than the ‘concerted’ mechanism. Criticism of this solution is difficult because the authors provided no specific suggestion as to how it might work; the justification provided was the low rate of bypass reactions. Since the short-circuit rates they measured were 10-fold slower than those measured by other groups, this justification is somewhat weakened. The relatively rapid rates of generation of superoxide by the bc_1 complex (1–3% maximal rate) have been the subject of an extensive literature, in which SQ at the Q_o site has been considered as the reductant for O_2 ⁴⁹ (see Table 2, reaction a’). Similar rates are observed under anaerobic conditions, when the second electron is transferred to cyt *c* rather than to O_2 ^{45,51} (reaction a). It might therefore be fruitful to discuss mechanisms in which the SQ is generated as a natural component of the reaction mechanism, even under inhibited conditions, rather than to reject all such mechanisms. In order to decide between these options, we must look more carefully at possible constraints on short-circuit rates.

9.2 Coulombic Gating in a Sequential Mechanism

If the mechanism is sequential, and involves SQ in the distal domain, the value of k_{cat} calculated for reduction of SQ by heme b_L^- is $\sim 5 \times 10^7$, which would match rates in the experimental range if occupancy was $\sim 10^{-8}$ SQ monomer⁻¹. We should note

however that if the SQ in the distal domain were at an occupancy in the $>10^{-4}$ range (required for rapid electron transfer in the forward direction from this domain), this short-circuit would be in the range $>10^3$ s⁻¹. That such bypass rates are not observed means that mechanisms with high SQ occupancy fail this critical test. It seems therefore that an explanation for the slow bypass rates observed in the context of the models involving SQ must be sought in terms of constraints that prevent the SQ from accessing the proximal domain *under circumstances in which heme b_L⁻ might be present*, while maintaining an occupancy $\leq 10^{-6}$ monomer⁻¹ in the distal domain.

The sequential mechanism previously suggested,^{53, 56, 93} involving a mobile SQ, provides a natural explanation for these otherwise paradoxical properties. To show how, we need to consider the fate of the second H⁺, and the interplay of charges in the site. The structures show that Glu-272 can occupy two different configurations. When involved in H-bonding with the distal domain occupant (stigmatellin in known structures, QH₂ initially in our model of the ES-complex), it points away from heme b_L. When not so involved, the side-chain rotates $>120^\circ$ so that the carboxylate group forms a H-bonding contact with a water molecule at the terminus of a water chain leading along the heme edge past one of the propionates to the P-phase water.^{56, 60, 105} A natural pathway for proton exit from the site involves transfer of the H⁺ from QH₂ (generated after the first electron transfer) to the Glu-272 carboxylate through the H-bond, to liberate the SQ anion, Q^{•-}. This would be followed by rotation of the Glu-272 side chain (now in the acid form) to the configuration in contact with the water chain, followed by release of H⁺ to allow exit to the P-phase.^{56, 85} In the configuration before rotation, Glu-272 and two H-bonded waters occupy most of the Q_c-site volume proximal to heme b_L. Rotation would open up the domain to occupancy by movement of Q^{•-} close to heme b_L. Rotation of Glu-272 and mobilization of Q^{•-}, with the potential for movement to the proximal domain, would therefore be linked processes:



(where subscripts *b* and *c* to ISPH indicate location at the *b*- and *c*-interfaces, respectively, and subscript *d* and *p* to SQ species indicate location in the distal and proximal domains of the Q_o site, respectively). In considering how this plays out in relation to bypass reactions, we need to take account of two effects:

- (i) The location of Q^{•-} would likely depend on the state of heme b_L. With the heme reduced, coulombic repulsion of Q^{•-} by heme b_L⁻ would favor location in the distal domain, and ensure that the Q^{•-} remained there unless the *oxidized* heme was available as an acceptor. With heme b_L oxidized, movement of Q^{•-} to the proximal domain to facilitate rapid electron transfer would be unconstrained, but a new set of coulombic interactions would couple the transfer of the electron on to heme b_H to release of the H⁺ from Glu-272 to the water chain.

- (ii) In order to reduce Q *via* heme b_L , reversal of the H^+ transfer would be necessary. Although the neutral Q could access the domain proximal to heme b_L^- without coulombic consequence, generation of Q^{*-} on reduction of Q by heme b_L^- would have obvious consequences on re-reduction of the heme. In addition, reduction by a second electron would not be favorable until protonation could occur (this sequence has been well characterized in the Q_B site of bacterial reaction centers¹⁰⁶), and this would require movement to the distal domain.

In general, the choreography of the second electron transfer in both directions will reflect the coulombic interactions between Q^{*-} , the glutamate carboxylate, the H^+ in the water chain, and the electron on heme b_L . The two effects above provide the constraints necessary to prevent excessive bypass rates, and with this natural extension of the hypothesis, the kinetic problems seem to be satisfactorily explained. Gating reflects both the coulombic effects, and the proton exchanges involving Glu-272. The gating is not to prevent formation of SQ, but to ensure that it is constrained to the distal domain unless heme b_L is oxidized (Figure 3, bottom).

9.3 Double Occupancy

Recent reports in favor of a double occupancy of the Q_o site by quinone have been reviewed elsewhere.^{52,84,107,108} Although this issue was not addressed by Osyczka *et al.*,³² a second quinone in the Q_o site could introduce rate constants that in principle would overcome the objections, developed above, to mechanisms in which the intermediate state from which the second electron transfers is constrained to the distal domain. By introducing an additional redox center in the otherwise too long path, rate constants in both directions could be raised by $>10^3$. However, the kinetic arguments³² leading to rapid short-circuits would then apply, giving bypass rates much greater than those observed. The double-occupancy solution therefore seems untenable for reactions involving a SQ intermediate in the distal domain.

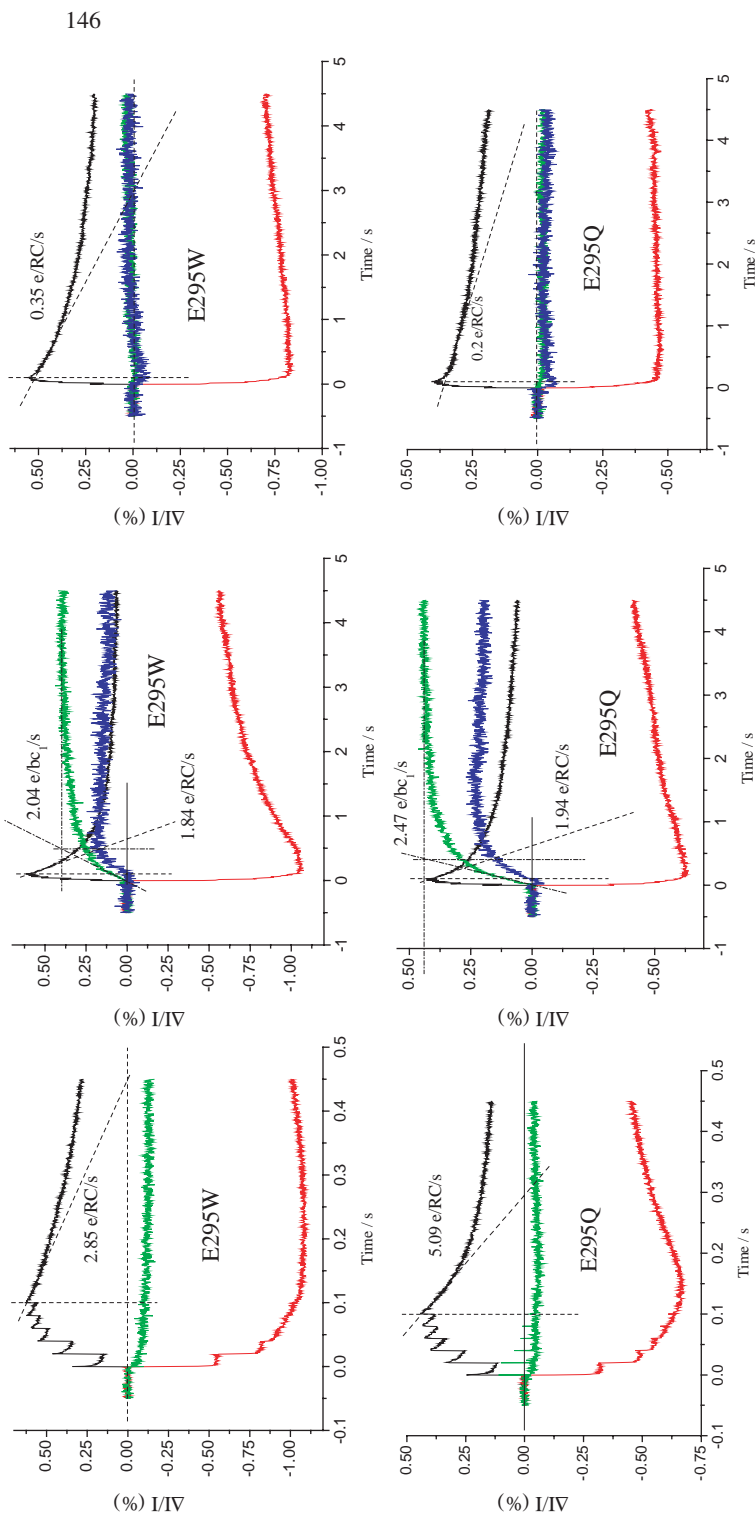
9.4 Location of the ES Complex or Activated State at Some Alternative Position

As noted above, the difficulties in accounting for the rates observed arise from the postulated location of the ES-complex at the distal domain, constrained by its H-bonds. Hong *et al.*⁹³ overcame these problems by allowing the SQ to move. An alternative is to suggest that the ES complex is located elsewhere and that the Q_o site reaction occurs through a 'concerted' process. In the reaction proposed,³² both electron transfers would have to occur from a state with no SQ property, at the top of the activation barrier, and with both electrons leaving within a single vibrational frequency. This would preclude nuclear movement, so both electrons would have to transfer from the same position. By locating the intermediate state halfway between ISP_{ox} and heme b_L ($R = 9.6 \text{ \AA}$, giving $k_o \sim 2.25 \times 10^9$), and assuming that $\Delta G^{0'}$ ~ 0 for both electron transfers, and that $\lambda \sim 4\Delta G^\ddagger \cong 2.0 \text{ V}$, the $k_{cat} \leq 1.5 \times 10^3 \text{ s}^{-1}$ calculated (using the Moser–Dutton term) provides the rate observed. There are five problems with this scenario. The first is that such a location has no structural justification. The second is the difficulty of accounting for

the linked H^+ transfers that must occur. The third is the abundant evidence that, in contrast to the expectations of this mechanism, short-circuits do occur. The fourth is the experimental evidence showing that the first electron transfer, but not the second, is rate limiting, as discussed above. Finally, Kramer and colleagues,¹⁰⁹ in a detailed study of the yeast bc_1 complex, have shown that electron transfer in the absence (normal forward QH_2 oxidation) and presence (bypass reaction) of antimycin showed essentially the same activation barriers and kinetic isotope effects. The characteristics strongly suggested that both involved the same mechanism, generation of a SQ intermediate at low occupancy.

10 Studies Using Glu-272 Mutants to Explore the Role of This Residue in Control of the Q_o site Reaction and Protection Against Excess ROS Production

The critical role we have suggested for Glu-272 in the mechanism of the Q_o site reaction can be tested by mutagenesis. Effects predicted from the above hypothesis are: (i) an involvement in the binding of stigmatellin, (ii) an involvement in binding of QH_2 (but not Q), and (iii) a critical role in transfer of the second electron. We have previously reported experimental evidence in favor of some of these effects on mutation of Glu-295, the equivalent residue in *Rb. sphaeroides*, to glutamine, aspartate or glycine.⁵⁶ The overall electron transfer was slowed, the binding constant for QH_2 was lowered (K_m was increased), and the site became weakly resistant to stigmatellin. Moreover, in the two most inhibited strains (E295G, E295Q) a normal $g_x = 1.80$ line was seen in the EPR spectrum of ISPH, indicating that its interaction with Q at the distal domain could still occur. From these results, we concluded that in the forward reaction, it might still be possible for the ES complex to form in these mutant strains, but that further progress would be blocked by inhibition of the second electron transfer, and by the strongly endergonic nature of the first electron transfer reaction. We have more recently constructed additional mutants at this site, and assayed these strains to explore the role of this residue further (see Figure 5 for example traces). In these experiments, chromatophores were suspended under aerobic conditions in a reaction medium containing 1 mM sodium ascorbate as reductant, and 1 mM potassium cyanide to block cyt *c* oxidase activity. Redox mediators were omitted to avoid their contribution to electron transfer. Valinomycin and nigericin were added so as to minimize the development of any proton gradient or contribution to absorbance changes from electrochromic effects. In a series of experiments with each strain, electron transfer kinetics of cyt c_1 plus c_2 , hemes b_H and b_L , and the reaction center (BChl) $_2^+$ (RC) were followed after one or six saturating actinic flashes. The experiments were performed in the absence of inhibitors (left column), in the presence of antimycin (middle column), or in the presence of both antimycin and myxothiazol (right column). In the presence of antimycin, activation by six flashes fully oxidized the high potential chain, and introduced several additional QH_2 into the pool, to set up conditions for maximal 'oxidant-induced reduction of cyt *b*'.¹¹⁰ These are also the conditions for maximal bypass activity at the Q_o site, assayed through the rate of reduction of RC. In *Rb. sphaeroides*, myxothiazol eliminates >90% of this activity,



Chapter 6

Figure 5 Kinetic traces showing measurement of bypass reactions in *Glu-295* mutant strains. Top, *E295W* strain; bottom, *E295Q* strain. The green traces show kinetics measured at 561–569 nm, to assay heme b_H reduction (upward deflection), with minor contributions from cyt c_1 plus c_2 subtracted; the black traces were measured at 542 nm to assay RC oxidation (upward deflection) and reduction; the red traces show heme b_L reduction (upward deflection), measured at 566–575, with contributions from heme b_H , RC, and cyt c_1 subtracted. The left hand column shows electron transfer in the absence of inhibitor; the middle column in the presence of antimycin (10 μ M), and the right column with antimycin (10 μ M) and myxothiazol (5 μ M). Valinomycin and nigericin (both at 5 μ M) were present throughout to allow rapid equilibration of the proton gradient, and traces were measured in a chromatophore suspension containing 0.5 μ M RC in 50 mM MOPS, 100 mM KCl at pH 7.0

so the right-hand traces show this myxothiazol-insensitive component. Much of this residual activity can be attributed to back reactions of RC. All mutant strains showed inhibited electron transfer through the Q_o site, as assayed either by re-reduction of RC in the absence of inhibitor, or by reduction of heme b_H in the presence of antimycin. However, all strains also showed rates for bypass reactions that accounted for a substantial fraction of the residual turnover of the site (Table 3). These were in some cases in excess of bypass rates in the wild type. These results show clearly that the first electron transfer could still occur to generate SQ, but that the second electron transfer is inhibited when Glu-295 is mutated. Furthermore, the slowed reduction of heme b_H in the mutant strains shows that SQ formed in the distal end of the Q_o site cannot transfer electrons to heme b_L at a normal rate. Since the distance is that from the distal domain discussed above, it seems clear that at this occupancy, the actual rate constant is too low. However, the rate constant estimated from the distance (as discussed above) is of about the right magnitude to account for the slow rates observed. It is noteworthy in the kinetic traces, but especially apparent in the presence of antimycin, that the mass action effects expected from the equilibrium constants operating within the separate chains, and between these and the Q pool catalyzed through the bifurcated reaction, are always in evidence. In the highly inhibited mutants, the consequence is that the quasi-equilibrium condition is not yet attained until some time after the last of the six flashes, so that the *b*-hemes continue to be reduced in the dark. In the seconds ensuing after maximal reduction is attained, the relaxation shows the pattern expected from the equilibria discussed in the introductory sections above; the reversible bifurcated reaction is still at play, but with much reduced rate constants. This is nicely explained by the hypothesis above; the SQ is now constrained to the distal domain, and movement of SQ (or Q) in the site has been lost, and with that, so have the rapid rates in both forward and reverse directions.

11 Conclusions

The critical problems identified by Osyczka *et al.*³² certainly apply to mechanisms that invoke a SQ intermediate and restrict it to the distal domain of the Q_o site. However, one of the solutions they propose, the ‘concerted’ reaction, seems quite improbable, and the doubly gated mechanism that prevents any SQ from accumulating seems tenable only with additional *ad hoc* hypotheses to explain the bypass reactions. On the other hand, the sequential mechanism we have proposed,⁵⁶ in which an intermediate semiquinone is transiently formed during ubihydroquinone oxidation, but can move within the Q_o site, can provide a satisfactory explanation for the properties observed. The gating functions discussed above represent a natural extension of the original hypothesis. Conclusions as to the demise of such hypotheses therefore seem premature. Notwithstanding the obvious utility of the Moser–Dutton approach,^{88–90} and the elegant simplification of electron transfer kinetics in the context of distance, our understanding of the Q_o site reactions has advanced through recognition of paradoxes revealed when application of the equations have showed an apparent contradiction with observed rates. A paradox has been defined as ‘Truth standing on her head to get attention’,¹¹¹ and this seems an appropriate take-home lesson from the above. The movement of the ISP extrinsic domain, the slowness of the rate-limiting step in relation

to the distance for electron transfer, and the difficulty in explaining rates pointed out by Osyczka *et al.*³² all appear paradoxical, but can be explained by mobility or recognition of reaction complexity.^{53, 112} The roadmaps provided by successful paradigms are the very stuff of science, but new understanding sometimes evolves when we are forced to look again.

Although the mechanism of the Q_o site seems well explained, several other areas remain controversial. The H-bonding of quinone at the Q_i site varies between structures.^{61, 66, 68} Different crystal-packing forces could possibly stabilize configurations involved in different stages of the catalytic cycle.¹¹³ The liganding of the relatively stable SQ at this site has been explored by high-resolution pulsed EPR and ENDOR, but again with differences, this time between species (^{68, 113} and F. MacMillan, personal communication). Since an understanding of the liganding is needed before a detailed mechanism can be justified, this controversy is still unresolved. Another critical question is that of electron transfer between monomers. Application of the Moser–Dutton equation to the dimeric structures suggests that electron transfer between the b_L hemes should be rapid.^{32, 69} This would allow both Q_o sites to communicate with both Q_i sites, so that in the presence of excess antimycin, titration of the Q_o site activity through inhibition of heme b_H reduction using myxothiazol or stigmatellin would give rise to strongly convex titration curves. In our hands, although the convex titration curves expected could be obtained when delivery of substrates was limiting, the titrations were linear when QH_2 was saturating. The convexity under limiting conditions seems better explained by a model of the sort suggested by Kroger and Klingenberg.¹¹⁴ Perhaps this is another paradox. Other kinetic experiments on mitochondrial complexes have been interpreted as showing dramatic interactions both across the dimer interface, and between the Q_o and Q_i sites,^{14,70,115} which seem in contradiction to the experimental data in the bacterial systems^{1,4,31,32} and the simple model discussed above. Further work will be needed to sort out this apparent discrepancy between mitochondrial and bacterial complexes.

Acknowledgements

Although the views expressed here are my own, they have been formed in the context of useful discussions with many colleagues, in particular Les Dutton, David Kramer, Peter Rich, Colin Wraight, Vlad Shinkarev, Ed Berry, Sergei Dikanov, Fraser MacMillan, and Fevzi Daldal. Support for research on the bc_1 complex from grant RO1 GM035438 from NIH is also gratefully acknowledged.

References

1. A.R. Crofts, S.W. Meinhardt, K.R. Jones, *et al.*, *Biochim. Biophys. Acta*, 1983, **723**, 202.
2. P. Mitchell, *FEBS Lett.*, 1975, **56**, 1.
3. P. Mitchell, *J. Theor. Biol.*, 1976, **62**, 327.
4. A.R. Crofts, *Photosynth. Res.*, 2003, **80**, 223.
5. D. Xia, C.-A. Yu, H. Kim, *et al.*, *Science*, 1997, **277**, 60.
6. Z. Zhang, L.-S. Huang, V.M. Shulmeister, *et al.*, *Nature (Lond.)*, 1998, **392**, 677.

7. S. Iwata, J.W. Lee, K. Okada, *et al.*, *Science*, 1998, **281**, 64.
8. E. Berry, M. Guergova-Kuras, L.-S. Huang, *et al.*, *Annu. Rev. Biochem.* 2000, **69**, 1007.
9. C. Hunte, S. Solmaz and C. Lange, *Biochim. Biophys. Acta* 2002, **1555**, 21.
10. C. Hunte, H. Palsdottir and B.L. Trumpower, *FEBS Lett.* 2003, **545**, 39.
11. H. Kim, D. Xia, C.A. Yu, *et al.*, *Proc. Natl. Acad. Sci. (U.S.)* 1998, **95**, 8026.
12. B.L. Trumpower, (2002).
13. K. Xiao, G. Engstrom, S. Rajagukguk, *et al.*, *J. Biol. Chem.* 2003, **278**, 11419.
14. C.-A. Yu, X. Wen, K. Xiao, *et al.*, *Biochim. Biophys. Acta* 2002, **1555**, 65.
15. A.R. Crofts and C.A. Wraight, *Biochim. Biophys. Acta* 1983, **726**, 149.
16. P.L. Dutton and D.M. Wilson, *Methods Enzymol.* 1976, **54**, 411.
17. A.R. Crofts and Z. Wang, *Photosynth. Res.* 1989, **22**, 69.
18. A.R. Crofts, in *The Enzymes of Biological Membranes*, Vol. 4, A.N. Martonosi(ed.) Plenum Publ. Corp., New York., 1985, 347.
19. S.W. Meinhardt and A.R. Crofts, *FEBS Lett.* 1982, **149**, 217.
20. S.W. Meinhardt and A.R. Crofts, *FEBS Lett.* 1982, **149**, 223.
21. S.W. Meinhardt and A.R. Crofts, *Biochim. Biophys. Acta* 1983, **723**, 219.
22. E.G. Glaser and A.R. Crofts, *Biochim. Biophys. Acta* 1984, **766**, 322.
23. E.G. Glaser, S.W. Meinhardt, and A.R. Crofts, *FEBS Lett.* 1984, **178**, 336.
24. M. Snozzi and A.R. Crofts, *Biochim. Biophys. Acta* 1984, **766**, 451.
25. M. Snozzi and A.R. Crofts, *Biochim. Biophys. Acta* 1985, **809**, 260.
26. P.R. Rich, *Biochim. Biophys. Acta* 1984, **768**, 53.
27. B.L. Trumpower, *Biochim Biophys Acta* 1981, **639**, 129.
28. J.R. Bowyer and A.R. Crofts, *Biochim. Biophys. Acta* 1981, **636**, 218.
29. P.B. Garland, R.A. Clegg, D. Boxer, *et al.*, in *Electron Transfer Chains and Oxidative Phosphorylation*, E. Quagliariello, S. Papa, F. Palmieri, E. C. Slater and N. Siliprandi (eds.), North-Holland Publishing Co., Amsterdam, The Netherlands., 1975, 351.
30. A.R. Crofts and S.W. Meinhardt, *Biochem. Soc. Trans.* 1982, **10**, 201.
31. A.R. Crofts, V.P. Shinkarev, D.R.J. Kolling, *et al.*, *J. Biol. Chem.* 2003, **278**, 36191.
32. A. Osyczka, C.C. Moser, Daldal, F. and P.L. Dutton, *Nature* 2004, **427**, 607.
33. V.P. Shinkarev, A.R. Crofts, and C.A. Wraight, *Biochemistry* 2001, **40**, 12584.
34. C.-H. Yun, A.R. Crofts and R.B. Gennis, *Biochemistry* 1991, **30**, 6747.
35. P. Joliot, A. Vermeglio, and A. Joliot, *Biochim. Biophys. Acta* 1989, **975**, 336.
36. J. Lavergne, P. Joliot, and A. Vermeglio, *Biochim. Biophys. Acta* 1989, **975**, 347.
37. A.T.a.J. Verméglio, P., *Trends in Microbiol.* 1999, **7**, 435.
38. C. Jungas, J.-L. Ranck, J.-L. Rigaud, P. Joliot and A. Verméglio, *EMBO J.* 1999, **18**, 534–542.
39. A.R. Crofts, M. Guergova-Kuras and S. Hong, *Photosynth. Res.* 1998, **55**, 357.
40. A.R. Crofts, *Trends in Microbiol.* 2000, **8**, 105.
41. C. Siebert, P. Qian, D. Fotiadis, A. Engel, C.N. Hunter and P.A. Bullough, *EMBO J.* 2004, **23**, 690.
42. S. Scheuring, F. Francia, J. Busselez, B.A. Melandri, J.-L. Rigaud, and D. Lévy, *J. Biol. Chem.* 2004, **279**, 3620.
43. F. Francia, J. Wang, G. Venturoli, B.A. Melandri, W.P. Barz and D. Oesterhelt, *Biochemistry* 1999, **38**, 6834.

44. E.A. Berry, L.-S. Huang, L.K. Saechao, N.G. Pon, M. Valkova-Valchanova and F. Daldal, *Photosynth. Res.* 2004, **81**, 251.
45. Y. Chen, in *Ph.D. Thesis in Biophysics*, University of Illinois at Urbana-Champaign, 1989, 143.
46. Y. Chen and A.R. Crofts, in *Current Research in Photosynthesis*, Vol. III, M. Baltscheffsky (ed.), Kluwer Academic Publishers, Dordrecht/Boston/London., 1990, 287.
47. A. Boveris, *Methods Enzymol.* 1984, **105**, 429.
48. F. Muller, *J. Am. Aging Assoc.* 2000, **23**, 227.
49. J.F. Turrens, A. Alexandre, and A.L. Lehninger, *Arch. Biochem. Biophys.* 1985, **237**, 408.
50. F.L. Muller, A.G. Roberts, M.K. Bowman, *et al.*, *Biochemistry* 2003, **42**, 6493.
51. F. Muller, A.R. Crofts, and D.M. Kramer, *Biochemistry* 2002, **41**, 7866.
52. A.R. Crofts, *Annu. Rev. Physiol.*, 2004, **66**, 689.
53. A.R. Crofts, *Biochim. Biophys. Acta* 2004, **1655**, 77.
54. P.R. Rich, *Biochim. Biophys. Acta* 2004, **1658**, 165.
55. E.A. Berry and L.S. Huang, *FEBS Lett.* 2003, **555**, 13.
56. A.R. Crofts, S.J. Hong, N. Ugulava, *et al.*, *Proc. Natl. Acad. Sci. U.S.A.*, 1999, **96**, 10021.
57. A.R. Crofts, B. Barquera, R.B. Gennis, *et al.*, *Biochemistry* 1999, **38**, 15807.
58. S. Junemann, P. Heathcote and P.R. Rich, *J. Biol. Chem.* 1998, **273**, 21603.
59. Z.-L. Zhang, E.A. Berry, L.-S. Huang, *et al.*, *Subcell. Biochem.* 2000, **35**, 541.
60. C. Hunte, J. Koepke, C. Lange, *et al.*, *Structure*, 2000, **8**, 669.
61. X. Gao, X. Wen, L. Esser, *et al.*, *Biochemistry*, 2003, **42**, 9067.
62. H. Palsdottir, C.G. Lojero, B.L. Trumpower, *et al.*, *J. Biol. Chem.* 2003, **278**, 31303.
63. J.J. Kessl, B.B. Lange, T. Merbitz-Zahradnik, *et al.*, *J. Biol. Chem.* 2003, **278**, 31312.
64. C.-A. Yu, D. Xia, H. Kim, *et al.*, *Biochim. Biophys. Acta* 1998, **1365**, 151.
65. X. Gao, X. Wen, C.-A. Yu, *et al.*, *Biochemistry* 2002, **41**, 11692.
66. C. Lange, J.H. Nett, B.L. Trumpower, *et al.*, *EMBO J.* 2001, **23**, 6591.
67. R.I. Samoilova, D. Kolling, T. Uzawa, *et al.*, *J. Biol. Chem.* 2002, **277**, 4605.
68. S.A. Dikanov, R.I. Samoilova, D.R.J. Kolling, *et al.*, *J. Biol. Chem.* 2004, **279**, 15814.
69. A.R. Crofts and E.A. Berry, *Curr. Opinions in Struc. Biol.*, 1998, **8**, 501.
70. C. Lange and C. Hunte, *Proc. Natl. Acad. Sci. U.S.A.*, 2002, **99**, 2800.
71. A.R. Crofts, M. Guergova-Kuras, L.-S. Huang, *et al.*, *Biochemistry* 1999, **38**, 15791.
72. A.R. Crofts, S. Hong, Z. Zhang, *et al.*, *Biochemistry* 1999, **38**, 15827.
73. A.R. Crofts, E.A. Berry, R. Kuras, *et al.*, in *Photosynthesis: Mechanisms and Effects*, Vol. III, G. Garab (ed.) Kluwer Academic Publ., Dordrecht/Boston/London., 1998, 1481.
74. E. Darrouzet and F. Daldal, *Biochemistry* 2003, **42**, 1499.
75. E. Darrouzet, C.C. Moser, P.L. Dutton, *et al.*, *TIBS* 2001, **26**, 445.
76. K. Xiao, L. Yu and C.A. Yu, *J. Biol. Chem.* 2000, **275**, 38597.

77. C.H. Snyder, E.B. Gutierrez-Cirlos and B.L. Trumpower, *J. Biol. Chem.* 2000, **275**, 13535.
78. H. Tian, L. Yu, M. W. Mather, *et al.*, *J. Biol. Chem.* 1998, **273**, 27953.
79. H. Tian, S. White, L. Yu, *et al.*, *J. Biol. Chem.* 1999, **274**, 7146.
80. J.H. Nett, C. Hunte and B.L. Trumpower, *Eur. J. Biochem.* 2000, **267**, 5777.
81. D.E. Robertson, F. Daldal and P.L. Dutton, *Biochemistry* 1990, **29**, 11249.
82. C. Snyder and B.L. Trumpower, *Biochim. Biophys. Acta* 1998, **1365**, 125.
83. N.B. Ugulava and A.R. Crofts, *FEBS Lett.* 1998, **440**, 409.
84. H. Ding, D.E. Robertson, F. Daldal, *et al.*, *Biochemistry* 1992, **31**, 3144.
85. A.R. Crofts, M. Guergova-Kuras, R. Kuras, *et al.*, *Biochim. Biophys. Acta* 2000, **1459**, 456.
86. M. Guergova-Kuras, R. Kuras, N. Ugulava, *et al.*, *Biochemistry* 2000, **39**, 7436.
87. C.C. Moser, J.M. Keske, K. Warncke, R.S. Farid and P.L. Dutton, *Nature* 1992, **355**, 796.
88. C.C. Moser, C.C. Page, R. Farid and P.L. Dutton, *J. Bioenerg. Biomembranes* 1995, **27**, 263.
89. C.C. Moser, C.C. Page, X.X. Chen and P.L. Dutton, *J. Biol. Inorg. Chem.* 1997, **2**, 393.
90. C.C. Page, C.C. Moser, X.X. Chen, *et al.*, *Nature* 1999, **402**, 47.
91. R.A. Marcus and N. Sutin, *Biochim. Biophys. Acta* 1985, **811**, 265.
92. D. DeVault, *Q. Rev. Biophys.* 1980, **13**, 387.
93. S.J. Hong, N. Ugulava, M. Guergova-Kuras, *et al.*, *J. Biol. Chem.* 1999, **274**, 33931.
94. E. Denke, T. Merbitzshradnik, O.M. Hatzfeld, *et al.*, *J. Biol. Chem.* 1998, **273**, 9085.
95. T. Schröter, O.M. Hatzfeld, S. Gemeinhardt, *et al.*, *Eur. J. Biochem.* 1998, **255**, 100.
96. T.A. Link, *Adv. Inorg. Chem.* 1999, **47**, 83.
97. C. Colbert, M.M.-J. Couture, L.D. Eltis, *et al.*, *Structure* 2000, **8**, 1267.
98. G.M. Ullmann, L. Noodleman and D.A. Case, *J. Biol. Inorg. Chem.* 2002, **7**, 632.
99. Y. Zu, M.M.-J., M.M.-J. Couture, *et al.*, *Biochemistry* 2003, **42**, 12400.
100. R.I. Cukier, *Biochim. Biophys. Acta* 2004, **1655**, 37.
101. C.J. Chang, M.C.Y. Chang, N.H. Damrauer and D.G. Nocera, *Biochim. Biophys. Acta* 2004, **1655**, 13.
102. T.A. Link, *FEBS Lett.* 1997, **412**, 257.
103. A.R. Crofts, V.P. Shinkarev, S.A. Dikanov, *et al.*, *Biochim. Biophys. Acta* 2002, **1555**, 48.
104. V.P. Shinkarev, D.R.J. Kolling, T.J. Miller, *et al.*, *Biochemistry* 2002, **41**, 14372.
105. S. Izrailev, A.R. Crofts, E.A. Berry, *et al.*, *Biophys. J.* 1999, **77**, 1753.
106. C.A. Wraight, *Frontiers in Bioscience* 2004, **9**, 309.
107. S. Bartoschek, M. Johansson, B.H. Geierstanger, *et al.*, *J. Biol. Chem.* 2001, **276**, 35231.
108. H. Ding, C.C. Moser, D.E. Robertson, *et al.*, *Biochemistry* 1995, **34**, 15979.

109. D.M. Kramer, J.L. Cape, I. Forquer, F. Muller and M.K. Bowman, submitted (2005).
110. E.C. Slater, in *Chemiosmotic Proton Circuits in Biological membranes*, V.P. Skulachev and P.C. Hinkle (ed.), Addison-Wesley Publ. Co., Reading, Mass., 1981, 69.
111. G.K. Chesterton, in *The Paradoxes of Mr. Pond* (Dover Books, 1937).
112. V.L. Davidson, *Biochemistry* 1996, **35**, 14036.
113. D.R.J. Kolling, R.I. Samoilova, J.T. Holland, *et al.*, *J. Biol. Chem.* 2003, **278**, 39747.
114. A. Kroger and M. Klingenberg, *Eur. J. Biochem.* 1973, **34**, 358.
115. R. Covian, E.B. Gutierrez-Cirlos and B.L. Trumpower, *J. Biol. Chem.* 2004, **279**, 15040.
116. G. Engstrom, K. Xiao, C.-A. Yu, *et al.*, *J. Biol. Chem.* 2002, **277**, 31072.
117. B. Hacker, B. Barquera, A.R. Crofts, *et al.*, *Biochemistry* 1993, **32**, 4403.
118. A.R. Crofts, B. Barquera, G. Bechmann, *et al.*, in *Photosynthesis: From Light to Biosphere.*, Vol. II, P. Mathis (ed.), Kluwer Academic Publ., Dordrecht., 1995, 493.
119. D.E. Robertson, R.C. Prince, J.R. Bowyer, *et al.*, *J. Biol. Chem.* 1984, **259**, 1758.
120. P.L. Dutton and J.B. Jackson, *Eur. J. Biochem.* 1972, **30**, 495.
121. J.R. Bowyer, S.W. Meinhardt, G.V. Tierney, *et al.*, *Biochim. Biophys. Acta* 1981, **635**, 167.
122. J.R. Bowyer, P.L. Dutton, R.C. Prince, *et al.*, *Biochim. Biophys. Acta* 1980, **592**, 445.
123. B. Hacker, B. Barquera, R.B. Gennis, *et al.*, *Biochemistry* 1994, **33**, 13022.
124. A.R. Crofts, B. Barquera, G. Bechmann, *et al.*, in *Photosynthesis: From Light to Biosphere.*, Vol. II, P. Mathis (ed.), Kluwer Academic Publ., Dordrecht., 1995, 493.
125. A.R. Crofts, http://www.life.uiuc.edu/crofts/Marcus_Bronsted/, 2004.

Appendix 1

Marcus Treatment of Endergonic Reactions

An alternative form of the Marcus equation has been suggested for treatment of endergonic processes [1], using the equation:

$$\log_{10} k_{\text{ct}}^{\text{end}} = 13.0 - 0.6(R - 3.6) - 3.1(-\Delta G + \lambda)^2/\lambda - \Delta G/0.06 \quad (\text{A.1})$$

In addition to what appears to be a conventional Marcus term, this equation seems to contain an extra Boltzmann term contributing to the energy barrier (the right-most term). This representation is misleading and unnecessary. The ‘additional term’ arises when estimating the activation barrier and rate-constant in the endergonic direction (which cannot be measured easily) using the reaction properties measured in the exergonic direction. It can be derived in its simplest form as follows (using electrical units for ΔG):

$$K_{\text{end}} = k_{\text{f}}^{\text{end}}/k_{\text{b}}^{\text{end}} = k_{\text{f}}^{\text{end}}/k_{\text{f}}^{\text{ex}} \quad (\text{A.2})$$

$$k_{\text{f}}^{\text{end}} = k_{\text{f}}^{\text{ex}} K_{\text{end}} \quad (\text{A.3})$$

$$\log_{10} k_{\text{f}}^{\text{end}} = \log_{10} k_{\text{f}}^{\text{ex}} + \log_{10} K_{\text{end}} = \log_{10} k_{\text{f}}^{\text{ex}} - \Delta G_{\text{end}}^0 / 2.303RT \quad (\text{A.4})$$

This expression can be extended using classical Marcus treatment [4, 5], and substitution using the Arrhenius expression, $k_{\text{f}}^{\text{ex}} = k_0 \exp(-\Delta G^{\#} \cdot F/RT)$, the Marcus term, $\Delta G^{\#} = (\Delta G^0 + \lambda)^2/4\lambda$, and the Moser *et al.* [2] expression for k_0 in terms of distance, R .

$$\log_{10} k_{\text{f}}^{\text{end}} = 13.0 - 0.6(R - 3.6) - \gamma(\Delta G_{\text{ex}}^0 + \lambda_{\text{ex}})^2/\lambda_{\text{ex}} - \Delta G_{\text{end}}^0 / 2.303RT \quad (\text{A.5})$$

The Moser–Dutton [1, 2] formulation, in which quantum-mechanical corrections modify the pre-exponential factor, has $\gamma = 3.1$ instead of 4.23. The Page *et al.* [1] version is then obtained by substituting $-\Delta G_{\text{end}}^0$ for ΔG_{ex}^0 . The λ used here is actually that for the exergonic reaction; the value is the same in both directions if the parabolas have the same shape (the same ‘spring constant’), but not otherwise.

An alternative treatment can be framed in terms of a set of Marcus parabolas [4, 5]. The endergonic energy barrier, $\Delta G_{\text{end}}^{\#}$, is calculated by adding $\Delta G_{\text{ex}}^{\#}$, the energy barrier in the exergonic direction, to the energy difference in the endergonic direction (the Boltzmann term in question). $\Delta G_{\text{ex}}^{\#}$ is estimated using the Marcus expression, with ΔG_{ex}^0 for the exergonic reaction direction, and a value for λ , λ_{ex} , obtained in principle from measurement of the exergonic rate. The tricky factor is again the replacement of ΔG_{ex}^0 by $-\Delta G_{\text{end}}^0$, its numerical equivalent. The underlying rate

equation in the endergonic direction has the same conventional Arrhenius form as that in the exergonic direction.

$$k_{\text{cat}} = k_0 \exp(-\Delta G_{\text{end}}^{\#}/RT) = k_0 \exp(-(\Delta G_{\text{ex}}^{\#} + \Delta G_{\text{end}}^0)/RT) \quad (\text{A.6})$$

Derivation of the Marcus term for $\Delta G^{\#}$ from Hooke's Law, using parabolas drawn to represent either the exergonic or endergonic direction, results in the same equation.

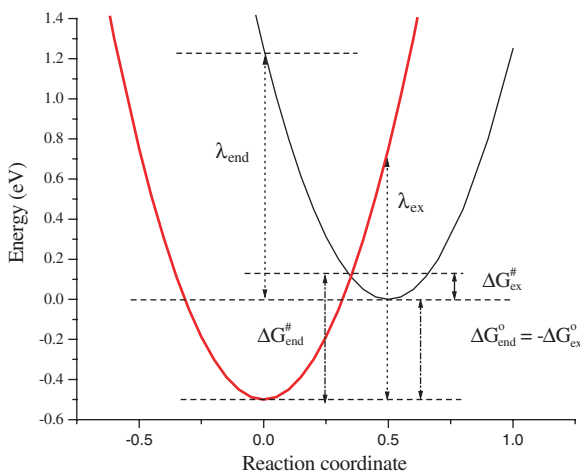


Figure A1 Marcus parabolas for an endergonic process, labeled to show the terms discussed in the text.

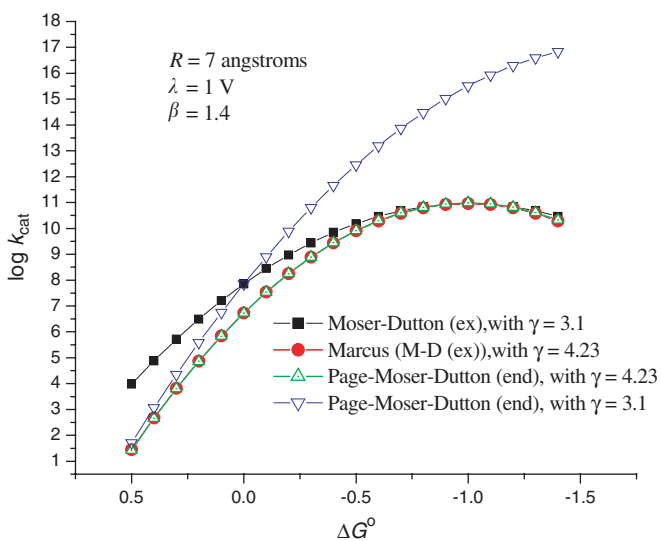


Figure A2 Curves showing the dependence of rate constant on driving force using different versions of the Moser-Dutton equation

The “additional Boltzmann term” of the Page *et al.* [1] equation is not an extra term contributing to the barrier, and the treatment used in (3) and this review, in which the endergonic region is treated using the standard Marcus term, is perfectly appropriate.

$$\log_{10} k_f^{\text{end}} = 13 - \frac{\beta}{2.303} (R - 3.6) - \gamma \frac{(\Delta G_{\text{end}}^0 + \lambda_{\text{end}})^2}{\lambda_{\text{end}}} \quad (\text{A.7})$$

The identity of the two equations can most easily be demonstrated by numerical substitution, as in Figure A2. Identical Marcus curves are generated using the exergonic or endergonic forms of the Page–Moser–Dutton equation, as long as a simple Marcus treatment (giving γ of 4.23 at 298 K) is used. However, it should be noted that with the Page *et al.* [1] equation, although $\Delta G_{\text{end}}^{\#}$ and $(\Delta G_{\text{ex}}^{\#} + \Delta G_{\text{end}}^0)$ have the same numerical value, the quantum mechanical correction implicit in $\gamma = 3.1$ is applied only to the part of this value corresponding to $\Delta G_{\text{ex}}^{\#}$. As a consequence, different values are generated for k_f^{end} when using the two equations, and the Marcus curve resulting from the treatment recommended in [1] (in which the ‘endergonic’ equation is used only for the endergonic part) shows a discontinuity in slope at the exergonic to endergonic transition, which is clearly unnatural.

References

1. C.C. Page, C.C. Moser, X. Chen, and P.L. Putton *Nature*, 1999 **402**, 47.
2. C.C. Moser, J.M. Keske, K. Warncke, R.S. Farid and P.L. Dutton, *Nature*, 1992, **355**, 796.
3. A.R. Crofts, *Biochim. Biophys. Acta*, 2004 **1655**, 77.
4. R. Marcus, *J. Chem. Phys.*, 1965 **43**, 679.
5. D. DeVault, *Q. Rev. Biophys.*, 1980 **13**, 387.